SUPPLEMENT TO
"EVALUATING POLICY INSTITUTIONS –150 YEARS OF US MONETARY POLICY–"

REGIS BARNICHON
Federal Reserve Bank of San Francisco and CEPR

GEERT MESTERS
Federal Reserve Bank of New York

Abstract We present the details for all proofs, provide additional empirical results, robustness checks and describe our proposed new instrument for identifying monetary shocks during the Gold Standard period. Section S1: Details and proofs, Section S2: Additional empirical results, Section S3: Robustness checks, Section S4: A new proxy for monetary policy shocks: large gold mine discoveries, 1879-1912

S1. DETAILS AND PROOFS

PROOF OF LEMMA 1: Define

$$\mathcal{A} = \begin{bmatrix} \mathcal{A}_{yy} & \mathcal{A}_{yp} \\ \mathcal{A}_{py} & \mathcal{A}_{pp} \end{bmatrix}, \ \mathcal{B} = \begin{bmatrix} \mathcal{B}_{y\xi} & 0 \\ \mathcal{B}_{p\xi} & \mathcal{B}_{p\epsilon} \end{bmatrix}, \ \mathbf{S} = \begin{bmatrix} \boldsymbol{\Xi} \\ \boldsymbol{\epsilon} \end{bmatrix} \text{ and } \mathbf{Z} = \begin{bmatrix} \mathbf{Y} \\ \mathbf{P} \end{bmatrix}. \tag{S1}$$

The model (14) is equivalent to $\mathcal{A}\mathbf{Z} = \mathcal{B}\mathbf{S}$. For any $\phi \in \Phi$ we have that there exists unique equilibrium representation. This implies that $\mathcal{A}$ is invertible and we obtain $\mathbf{Z} = \mathcal{D}\mathbf{S}$, with $\mathcal{D} = \mathcal{A}^{-1}\mathcal{B}$. The block structure of $\mathcal{D}$ is given by

$$\mathcal{D} = \begin{bmatrix} \Theta(\phi,\theta) \\ \Theta_p(\phi,\theta) \end{bmatrix} = \begin{bmatrix} \Gamma(\phi,\theta) & \mathcal{R}(\phi,\theta) \\ \Gamma_p(\phi,\theta) & \mathcal{R}_p(\phi,\theta) \end{bmatrix}.$$

Explicit expression can be obtained by by noting that $\mathcal{A}$ being invertible implies that $\mathcal{A}_{pp}$ and $\mathcal{A}_{yy} - \mathcal{A}_{yp}\mathcal{A}_{pp}^{-1}\mathcal{A}_{py}$ are invertible as $\mathcal{A}_{yy}$ is generally not invertible. We have

$$\begin{bmatrix} \Gamma(\phi,\theta) & \mathcal{R}(\phi,\theta) \\ \Gamma_p(\phi,\theta) & \mathcal{R}_p(\phi,\theta) \end{bmatrix} = \begin{bmatrix} \mathcal{V}(\mathcal{B}_{y\xi} - \mathcal{A}_{yp}\mathcal{A}_{pp}^{-1}\mathcal{B}_{p\xi}) & -\mathcal{V}\mathcal{A}_{yp}\mathcal{A}_{pp}^{-1}\mathcal{B}_{p\epsilon} \\ -\mathcal{A}_{pp}^{-1}\mathcal{A}_{py}\mathcal{V}\mathcal{B}_{y\xi} + (\mathbf{I} + \mathcal{A}_{pp}^{-1}\mathcal{A}_{py}\mathcal{V}\mathcal{A}_{yp})\mathcal{A}_{pp}^{-1}\mathcal{B}_{p\xi} & (\mathbf{I} + \mathcal{A}_{pp}^{-1}\mathcal{A}_{py}\mathcal{V}\mathcal{A}_{yp})\mathcal{A}_{pp}^{-1}\mathcal{B}_{p\epsilon} \end{bmatrix} \tag{S2}$$

with $\mathcal{V} = (\mathcal{A}_{yy} - \mathcal{A}_{yp}\mathcal{A}_{pp}^{-1}\mathcal{A}_{yp})^{-1}$. *Q.E.D.*

PROOF OF LEMMA 2: Given some $\phi \in \Phi$ we can follow the same steps as the proof of Lemma 1 but using an augmented policy rule

$$\mathcal{A}_{pp}\mathbf{P} - \mathcal{A}_{py}\mathbf{Y} = (\mathcal{B}_{p\xi} + \mathcal{B}_{p\epsilon}\mathcal{T}_\xi)\boldsymbol{\Xi} + (\mathcal{B}_{p\epsilon} + \mathcal{B}_{p\epsilon}\mathcal{T}_\epsilon)\boldsymbol{\epsilon}.$$

Replacing $\mathcal{B}_{p\xi}$ by $\mathcal{B}_{p\xi} + \mathcal{B}_{p\epsilon}\mathcal{T}_\xi$ and $\mathcal{B}_{p\epsilon}$ by $\mathcal{B}_{p\epsilon} + \mathcal{B}_{p\epsilon}\mathcal{T}_\epsilon$ in (S2), allows to write

$$\begin{bmatrix} \mathbf{Y} \\ \mathbf{P} \end{bmatrix} = \begin{bmatrix} \Gamma(\phi,\theta) + \mathcal{R}(\phi,\theta)\mathcal{T}_\xi & \mathcal{R}(\phi,\theta) + \mathcal{R}(\phi,\theta)\mathcal{T}_\epsilon \\ \Gamma_p(\phi,\theta) + \mathcal{R}_p(\phi,\theta)\mathcal{T}_\xi & \mathcal{R}_p(\phi,\theta) + \mathcal{R}_p(\phi,\theta)\mathcal{T}_\epsilon \end{bmatrix} \begin{bmatrix} \boldsymbol{\Xi} \\ \boldsymbol{\epsilon} \end{bmatrix}, \tag{S3}$$

Regis Barnichon: Regis.Barnichon@sf.frb.org
Geert Mesters: geert.mesters@ny.frb.org

which can also be written as

$$\mathbf{Y} = (\Theta(\phi,\theta) + \mathcal{R}(\phi,\theta)\mathcal{T})\mathbf{S} \qquad \text{and} \qquad \mathbf{P} = (\Theta_p(\phi,\theta) + \mathcal{R}_p(\phi,\theta)\mathcal{T})\mathbf{S}\ .$$

We obtain Lemma 2 for $\phi = \phi^0$. *Q.E.D.*

PROOF OF LEMMA 3: We start by showing $\mathcal{L}^{\text{opt}} = \mathsf{L}(\mathcal{T}^*;\phi^0,\theta)$. To do so, we proceed mechanically and show $\{\min_\phi \mathcal{L} \text{ s.t. } (14)\} = \{\min_\mathcal{T} \mathsf{L}(\mathcal{T};\phi^0,\theta) \text{ s.t. } (14) \text{ with } \mathcal{A}_{pp} = \mathcal{A}^0_{pp},\ \mathcal{A}_{py} = \mathcal{A}^0_{py}, \mathcal{B}_{p\xi} = \mathcal{B}^0_{p\xi},\ \mathcal{B}_{p\epsilon} = \mathcal{B}^0_{p\epsilon}\}$. Note that $\mathbf{Y}$ can be written as $\mathbf{Y} = (\mathcal{V}\mathcal{B}_{y\xi} - \mathcal{V}\mathcal{A}_{yp}\mathcal{A}^{-1}_{pp}\mathcal{B}_{p\xi})\mathbf{\Xi} - \mathcal{V}\mathcal{A}_{yp}\mathcal{A}^{-1}_{pp}\mathcal{B}_{p\epsilon}\boldsymbol{\epsilon}$ Using that the entries of $\mathbf{\Xi}$ and $\boldsymbol{\epsilon}$ have mean zero, unit variance and are uncorrelated we have that

$$\begin{aligned}\mathcal{L} =& \mathbb{E}(\mathbf{Y}'\mathcal{W}\mathbf{Y})\\ =& \text{Tr}((\mathcal{B}_{y\xi} - \mathcal{A}_{yp}\mathcal{A}^{-1}_{pp}\mathcal{B}_{p\xi})'\mathcal{V}'\mathcal{W}\mathcal{V}(\mathcal{B}_{y\xi} - \mathcal{A}_{yp}\mathcal{A}^{-1}_{pp}\mathcal{B}_{p\xi}))\\ &+ \text{Tr}((\mathcal{V}\mathcal{A}_{yp}\mathcal{A}^{-1}_{pp}\mathcal{B}_{p\epsilon})'\mathcal{W}\mathcal{V}\mathcal{A}_{yp}\mathcal{A}^{-1}_{pp}\mathcal{B}_{p\epsilon})\ .\end{aligned}$$

Regardless of the values of $\{\mathcal{A}_{pp}, \mathcal{A}_{py}, \mathcal{B}_{p\xi}\}$ the optimal solution for $\mathcal{B}_{p\epsilon}$ satisfies $\mathcal{B}^{\text{opt}}_{p\epsilon} = \mathbf{0}$. After setting $\mathcal{B}_{p\epsilon} = \mathcal{B}^{\text{opt}}_{p\epsilon}$ the derivative maps of $\mathcal{L}$ with respect to $\{\mathcal{A}_{pp}, \mathcal{A}_{py}, \mathcal{B}_{p\xi}\}$ are given by

$$\begin{aligned}\mathcal{A}^{-1'}_{pp}\mathcal{A}'_{yp}\mathcal{V}'\mathcal{W}\mathcal{V}(\mathcal{B}_{y\xi} - \mathcal{A}_{yp}\mathcal{A}^{-1}_{pp}\mathcal{B}_{p\xi})\mathcal{B}'_{p\xi}\mathcal{A}^{-1'}_{pp} +&\\ \mathcal{A}^{-1'}_{pp}\mathcal{A}'_{yp}\mathcal{V}'\mathcal{W}\mathcal{V}(\mathcal{B}_{y\xi} - \mathcal{A}_{yp}\mathcal{A}^{-1}_{pp}\mathcal{B}_{p\xi})(\mathcal{B}_{y\xi} - \mathcal{A}_{yp}\mathcal{A}^{-1}_{pp}\mathcal{B}_{p\xi})'\mathcal{V}'\mathcal{A}'_{py}\mathcal{A}^{-1'}_{pp} &= \mathbf{0}\\ \mathcal{A}^{-1'}_{pp}\mathcal{A}'_{yp}\mathcal{V}'\mathcal{W}\mathcal{V}(\mathcal{B}_{y\xi} - \mathcal{A}_{yp}\mathcal{A}^{-1}_{pp}\mathcal{B}_{p\xi})(\mathcal{B}_{y\xi} - \mathcal{A}_{yp}\mathcal{A}^{-1}_{pp}\mathcal{B}_{p\xi})'\mathcal{V}' &= \mathbf{0}\\ \mathcal{A}^{-1'}_{pp}\mathcal{A}'_{yp}\mathcal{V}'\mathcal{W}\mathcal{V}(\mathcal{B}_{y\xi} - \mathcal{A}_{yp}\mathcal{A}^{-1}_{pp}\mathcal{B}_{p\xi}) &= \mathbf{0}\end{aligned}$$

The last equation gives the derivative map with respect to $\mathcal{B}_{p\xi}$. Solving this expression for $\mathcal{B}_{p\xi}$ yields

$$\mathcal{B}^{\text{opt}}_{p\xi} = [\mathcal{A}^{-1'}_{pp}\mathcal{A}'_{yp}\mathcal{V}'\mathcal{W}\mathcal{V}\mathcal{A}_{yp}\mathcal{A}^{-1}_{pp}]^{-1}\mathcal{A}^{-1'}_{pp}\mathcal{A}'_{yp}\mathcal{V}'\mathcal{W}\mathcal{V}\mathcal{B}_{y\xi}\ .$$

Further, it is easy to see that if the last equation holds then the first two equations also hold. This holds regardless of $\mathcal{A}_{pp}$ and $\mathcal{A}_{py}$ as long as the invertibility conditions above are satisfied. It remains to show that $\mathcal{B}^{\text{opt}}_{p\xi} = \mathcal{B}^0_{p\xi} + \mathcal{B}^0_{p\epsilon}\mathcal{T}^*_\xi$ and $\mathcal{B}^{\text{opt}}_{p\epsilon} = \mathcal{B}^0_{p\epsilon} + \mathcal{B}^0_{p\epsilon}\mathcal{T}^*_\epsilon$, where $\mathcal{T}^* = (\mathcal{T}^*_\xi, \mathcal{T}^*_\epsilon) = -(\mathcal{R}^{0'}\mathcal{W}\mathcal{R}^0)^{-1}\mathcal{R}^{0'}\mathcal{W}(\Gamma^0, \mathcal{R}^0)$. The latter is straightforward as $\mathcal{T}^*_\epsilon = -\mathbf{I}$. For the former we have

$$\begin{aligned}&\mathcal{B}^0_{p\xi} + \mathcal{B}^0_{p\epsilon}\mathcal{T}^*_\xi\\ &= \mathcal{B}^0_{p\xi} - \mathcal{B}^0_{p\epsilon}(\mathcal{R}^{0'}\mathcal{W}\mathcal{R}^0)^{-1}\mathcal{R}^{0'}\mathcal{W}\Gamma^0\\ &= \mathcal{B}^0_{p\xi} + \mathcal{B}^0_{p\epsilon}((\mathcal{V}^0\mathcal{A}^0_{yp}(\mathcal{A}^0_{pp})^{-1}\mathcal{B}^0_{p\epsilon})'\mathcal{W}\mathcal{V}^0\mathcal{A}^0_{yp}(\mathcal{A}^0_{pp})^{-1}\mathcal{B}^0_{p\epsilon})^{-1}(\mathcal{V}^0\mathcal{A}^0_{yp}(\mathcal{A}^0_{pp})^{-1}\mathcal{B}^0_{p\epsilon})'\mathcal{W}\Gamma^0\\ &= \mathcal{B}^0_{p\xi} + ((\mathcal{V}^0\mathcal{A}^0_{yp}(\mathcal{A}^0_{pp})^{-1})'\mathcal{W}\mathcal{V}^0\mathcal{A}^0_{yp}(\mathcal{A}^0_{pp})^{-1})^{-1}(\mathcal{V}^0\mathcal{A}^0_{yp}(\mathcal{A}^0_{pp})^{-1})'\mathcal{W}\Gamma^0\\ &= \mathcal{B}^0_{p\xi} + ((\mathcal{V}^0\mathcal{A}^0_{yp}(\mathcal{A}^0_{pp})^{-1})'\mathcal{W}\mathcal{V}^0\mathcal{A}^0_{yp}(\mathcal{A}^0_{pp})^{-1})^{-1}(\mathcal{V}^0\mathcal{A}^0_{yp}(\mathcal{A}^0_{pp})^{-1})'\mathcal{W}\mathcal{V}^0\mathcal{B}_{y\xi}\\ &- ((\mathcal{V}^0\mathcal{A}^0_{yp}(\mathcal{A}^0_{pp})^{-1})'\mathcal{W}\mathcal{V}^0\mathcal{A}^0_{yp}(\mathcal{A}^0_{pp})^{-1})^{-1}(\mathcal{V}^0\mathcal{A}^0_{yp}(\mathcal{A}^0_{pp})^{-1})'\mathcal{W}\mathcal{V}^0\mathcal{A}_{yp}\mathcal{A}^{-1}_{pp}\mathcal{B}^0_{p\xi}\\ &= ((\mathcal{V}^0\mathcal{A}^0_{yp}(\mathcal{A}^0_{pp})^{-1})'\mathcal{W}\mathcal{V}^0\mathcal{A}^0_{yp}(\mathcal{A}^0_{pp})^{-1})^{-1}(\mathcal{V}^0\mathcal{A}^0_{yp}(\mathcal{A}^0_{pp})^{-1})'\mathcal{W}\mathcal{V}^0\mathcal{B}_{y\xi} = \mathcal{B}^{\text{opt}}_{p\xi}\ ,\end{aligned}$$

where the third equality uses that $\mathcal{B}^0_{p\epsilon}$ is invertible. *Q.E.D.*

PROOF OF PROPOSITION 1: Using Lemma 3 we have

$$\begin{aligned}\Delta &= \mathcal{L}^0 - \mathcal{L}^{\text{opt}} = \text{Tr}(\Theta^{0'}\mathcal{W}\Theta^0) - \text{Tr}((\Theta^0 + \mathcal{R}^0\mathcal{T}^*)'\mathcal{W}(\Theta^0 + \mathcal{R}^0\mathcal{T}^*)) \\ &= \text{Tr}(\Theta^{0'}\mathcal{W}\mathcal{R}^0(\mathcal{R}^{0'}\mathcal{W}\mathcal{R}^0)^{-1}\mathcal{R}^{0'}\mathcal{W}\Theta^0) = \sum_{s\in\mathcal{N}} \Theta_s^{0'}\mathcal{W}\mathcal{R}^0(\mathcal{R}^{0'}\mathcal{W}\mathcal{R}^0)^{-1}\mathcal{R}^{0'}\mathcal{W}\Theta_s^0 \,.\end{aligned}$$

For part 2, using Lemmas 2 and 3 we have

$$\Delta\Theta_p = \Theta_p^0 - \Theta_p^{\text{opt}} = \Theta_p^0 - (\Theta_p^0 + \mathcal{R}_p^0\mathcal{T}^*) = \mathcal{R}_p^0(\mathcal{R}^{0'}\mathcal{W}\mathcal{R}^0)^{-1}\mathcal{R}^{0'}\mathcal{W}\Theta^0 \,.$$

The sth column give the statement in the proposition. *Q.E.D.*

PROOF OF PROPOSITION 2: An explicit expressions for $\mathcal{T}_\mathcal{S}^* = (\mathcal{T}_{\xi,\mathcal{S}}, \mathcal{T}_{\epsilon,\mathcal{S}})$ is found by solving the linear quadratic problem

$$\begin{aligned}&\min_{\mathcal{T}_\mathcal{S}} \mathbb{E}(\mathbf{Y}'\mathcal{W}\mathbf{Y}) \quad \text{s.t.} \quad \mathbf{Y} = (\Gamma_\mathcal{S}^0 + \mathcal{R}_\mathcal{S}^0\mathcal{T}_{\xi,\mathcal{S}})\boldsymbol{\Xi}_\mathcal{S} + (\mathcal{R}_\mathcal{S}^0 + \mathcal{R}_\mathcal{S}^0\mathcal{T}_{\epsilon,\mathcal{S}})\boldsymbol{\epsilon}_\mathcal{S} + \Gamma_{-\mathcal{S}}^0\boldsymbol{\Xi}_{-\mathcal{S}} + \mathcal{R}_{-\mathcal{S}}^0\boldsymbol{\epsilon}_{-\mathcal{S}} \\ &= \min_{\mathcal{T}_\mathcal{S}} \text{Tr}[(\Theta_\mathcal{S}^0 + \mathcal{R}_\mathcal{S}^0\mathcal{T}_\mathcal{S})'\mathcal{W}(\Theta_\mathcal{S}^0 + \mathcal{R}_\mathcal{S}^0\mathcal{T}_\mathcal{S})]\end{aligned}$$

which is the equivalent of Lemma 3 when only adjusting $\mathcal{T}_\mathcal{S}$. For part 1, we use that $\mathcal{L}^0 = \text{Tr}(\Gamma^{0'}\mathcal{W}\Gamma^0) + \text{Tr}(\mathcal{R}^{0'}\mathcal{W}\mathcal{R}^0)$ and

$$\begin{aligned}\mathsf{L}(\mathcal{T}_\mathcal{S}^*;\phi^0,\theta) =& \text{Tr}((\Gamma_\mathcal{S}^0 + \mathcal{R}_\mathcal{S}^0\mathcal{T}_{\xi,\mathcal{S}}^*)'\mathcal{W}(\Gamma_\mathcal{S}^0 + \mathcal{R}_\mathcal{S}^0\mathcal{T}_{\xi,\mathcal{S}}^*)) \\ &+ \text{Tr}((\mathcal{R}_\mathcal{S}^0 + \mathcal{R}_\mathcal{S}^0\mathcal{T}_{\epsilon,\mathcal{S}}^*)'\mathcal{W}(\mathcal{R}_\mathcal{S}^0 + \mathcal{R}_\mathcal{S}^0\mathcal{T}_{\epsilon,\mathcal{S}}^*)) \\ &+ \text{Tr}(\Gamma_{-\mathcal{S}}^{0'}\mathcal{W}\Gamma_{-\mathcal{S}}^0) + \text{Tr}(\mathcal{R}_{-\mathcal{S}}^{0'}\mathcal{W}\mathcal{R}_{-\mathcal{S}}^0)\end{aligned}$$

Subtracting the two losses gives

$$\begin{aligned}\Delta_\mathcal{S}\mathcal{L} &= \mathcal{L}^0 - \mathsf{L}(\mathcal{T}_\mathcal{S}^*;\phi^0,\theta) = \text{Tr}[\Theta_\mathcal{S}^{0'}\mathcal{W}\mathcal{R}_\mathcal{S}^0(\mathcal{R}_\mathcal{S}^{0'}\mathcal{W}\mathcal{R}_\mathcal{S}^0)^{-1}\mathcal{R}_\mathcal{S}^{0'}\mathcal{W}\Theta_\mathcal{S}^0] \\ &= \sum_{s\in\mathcal{N}_\mathcal{S}} \Theta_s^{0'}\mathcal{W}\mathcal{R}_\mathcal{S}^0(\mathcal{R}_\mathcal{S}^{0'}\mathcal{W}\mathcal{R}_\mathcal{S}^0)^{-1}\mathcal{R}_\mathcal{S}^{0'}\mathcal{W}\Theta_s^0\end{aligned}$$

For part 2 we have

$$\Delta_\mathcal{S}\Theta_{\mathcal{S},p} = \Theta_{\mathcal{S},p}^0 - \Theta_{\mathcal{S},p}^{\text{opt}} = \Theta_{\mathcal{S},p}^0 - \Theta_{\mathcal{S},p}^0 - \mathcal{R}_{\mathcal{S},p}\mathcal{T}_\mathcal{S}^* = \mathcal{R}_{\mathcal{S},p}(\mathcal{R}_\mathcal{S}^{0'}\mathcal{W}\mathcal{R}_\mathcal{S}^0)^{-1}\mathcal{R}_\mathcal{S}^{0'}\mathcal{W}\Theta_\mathcal{S}^0 \,,$$

and the sth column of this expression gives the result.

Q.E.D.

PROOF OF LEMMA 4: The first part follows from

$$\begin{aligned}\min_\mathcal{T} \mathsf{L}(\mathcal{T};\phi^0,\theta) &= \min_\mathcal{T} \text{Tr}((\Theta^0 + \mathcal{R}^0\mathcal{T})'\mathcal{W}(\Theta^0 + \mathcal{R}^0\mathcal{T})) \\ &= \min_\mathcal{T} \text{Tr}((\Theta^0 + \mathcal{R}^0(\mathcal{R}_p^0)^{-1}\mathcal{R}_p^0\mathcal{T})'\mathcal{W}(\Theta^0 + \mathcal{R}^0(\mathcal{R}_p^0)^{-1}\mathcal{R}_p^0\mathcal{T})) \\ &= \min_{\Delta\Theta_p} \text{Tr}((\Theta^0 + \mathcal{R}^0(\mathcal{R}_p^0)^{-1}\Delta\Theta_p)'\mathcal{W}(\Theta^0 + \mathcal{R}^0(\mathcal{R}_p^0)^{-1}\Delta\Theta_p))\end{aligned}$$

as $\mathcal{R}_p^0$ is invertible. Similarly, for the second part note that $\mathcal{R}_{\mathcal{S}}^0 = \mathcal{R}^0\Omega_\epsilon'$ such that

$$\begin{aligned}
\min_{\mathcal{T}_{\mathcal{S}}} \mathsf{L}(\mathcal{T}_{\mathcal{S}};\phi^0,\theta) &= \min_{\mathcal{T}_{\mathcal{S}}} \mathrm{Tr}[(\Theta_{\mathcal{S}}^0 + \mathcal{R}_{\mathcal{S}}^0\mathcal{T}_{\mathcal{S}})'\mathcal{W}(\Theta_{\mathcal{S}}^0 + \mathcal{R}_{\mathcal{S}}^0\mathcal{T}_{\mathcal{S}})] \qquad \text{(S4)}\\
&= \min_{\mathcal{T}_{\mathcal{S}}} \mathrm{Tr}[(\Theta_{\mathcal{S}}^0 + \mathcal{R}_{\mathcal{S}}^0(\mathcal{R}_p^0)^{-1}\mathcal{R}_p^0\Omega_\epsilon'\mathcal{T}_{\mathcal{S}})'\mathcal{W}(\Theta_{\mathcal{S}}^0 + \mathcal{R}^0(\mathcal{R}_p^0)^{-1}\mathcal{R}_p^0\Omega_\epsilon'\mathcal{T}_{\mathcal{S}})]\\
&= \min_{\mathcal{T}_{\mathcal{S}}} \mathrm{Tr}[(\Theta_{\mathcal{S}}^0 + \mathcal{R}_{\mathcal{S}}^0(\mathcal{R}_p^0)^{-1}\mathcal{R}_{\mathcal{S},p}^0\mathcal{T}_{\mathcal{S}})'\mathcal{W}(\Theta_{\mathcal{S}}^0 + \mathcal{R}^0(\mathcal{R}_p^0)^{-1}\Delta\Theta_{\mathcal{S},p})]\\
&= \min_{\Delta\Theta_{\mathcal{S},p}\in\mathrm{col}(\mathcal{R}_{\mathcal{S},p}^0)} \mathrm{Tr}[(\Theta_{\mathcal{S}}^0 + \mathcal{R}_{\mathcal{S}}^0(\mathcal{R}_p^0)^{-1}\mathcal{R}_{\mathcal{S},p}^0\mathcal{T}_{\mathcal{S}})'\mathcal{W}(\Theta_{\mathcal{S}}^0 + \mathcal{R}^0(\mathcal{R}_p^0)^{-1}\Delta\Theta_{\mathcal{S},p})] \,.
\end{aligned}$$

Q.E.D.

PROOF OF PROPOSITION 3: Expression (S4) in the proof of Lemma 4 shows that if $\mathrm{col}(\mathcal{R}_{\mathcal{S},p}^j)$ is equal for $j = A, B$ the optimization problem no longer depends on Ω_ϵ for any non-policy shock. Specifically, note that $\Theta_{\mathcal{S}}^0 = [\Gamma_{\mathcal{S}}^0, \mathcal{R}_{\mathcal{S}}^0]$ and $\mathcal{R}_{\mathcal{S}}^0 = \mathcal{R}^0\Omega_\epsilon'$ which still depends on the weights Ω_ϵ, but the optimization problem for any Γ_s^0 component does not depend on Ω_ϵ. *Q.E.D.*

Before presenting the proofs of Corollaries 1, 2 and 3 we provide some additional details for the definition of the distance to minimum loss for the subset case where the reaction function is updated with respect to all policy shocks, but only along the policy paths that are identified by the subset of policy shocks. Following the main text we define the augmented policy rule

$$\mathcal{A}_{pp}^0\mathbf{P} - \mathcal{A}_{py}^0\mathbf{Y} = \mathcal{B}_{p\xi}^0\boldsymbol{\Xi} + \mathcal{B}_{p\epsilon}^0\boldsymbol{\epsilon} + \mathcal{B}_{p\epsilon}^0\Omega_\epsilon\widetilde{\mathcal{T}}_{\mathcal{S}}\mathbf{S} \,.$$

Under this rule the equilibrium, following the same steps that gave Lemma 2, becomes

$$\mathbf{Y} = (\Theta_0 + \mathcal{R}_{\mathcal{S}}^0\widetilde{\mathcal{T}}_{\mathcal{S}})\mathbf{S} \qquad \text{and} \qquad \mathbf{P} = (\Theta_p^0 + \mathcal{R}_{\mathcal{S},p}^0\widetilde{\mathcal{T}}_{\mathcal{S}})\mathbf{S}$$

Minimizing the loss wrt $\widetilde{\mathcal{T}}_{\mathcal{S}}$ gives

$$\begin{aligned}
\widetilde{\mathcal{T}}_{\mathcal{S}}^* &= \underset{\widetilde{\mathcal{T}}_{\mathcal{S}}}{\mathrm{argmin}}\, \mathsf{L}(\widetilde{\mathcal{T}}_{\mathcal{S}};\phi^0,\theta)\\
&= \underset{\widetilde{\mathcal{T}}_{\mathcal{S}}}{\mathrm{argmin}}\, \mathbb{E}(\mathbf{Y}'\mathcal{W}\mathbf{Y}) \qquad \text{s.t.} \quad \mathbf{Y} = (\Theta_0 + \mathcal{R}_{\mathcal{S}}^0\widetilde{\mathcal{T}}_{\mathcal{S}})\mathbf{S}\\
&= \underset{\widetilde{\mathcal{T}}_{\mathcal{S}}}{\mathrm{argmin}}\, \mathrm{Tr}[(\Theta^0 + \mathcal{R}_{\mathcal{S}}^0\widetilde{\mathcal{T}}_{\mathcal{S}})'\mathcal{W}(\Theta^0 + \mathcal{R}_{\mathcal{S}}^0\widetilde{\mathcal{T}}_{\mathcal{S}})]\\
&= -(\mathcal{R}_{\mathcal{S}}^{0\prime}\mathcal{W}\mathcal{R}_{\mathcal{S}}^0)^{-1}\mathcal{R}_{\mathcal{S}}^{0\prime}\mathcal{W}\Theta^0 \,.
\end{aligned}$$

The total subset distance to minimum loss is then

$$\begin{aligned}
\Delta_{\mathcal{S}}\mathcal{L} &= \mathcal{L}^0 - \mathsf{L}(\widetilde{\mathcal{T}}_{\mathcal{S}}^*;\phi^0,\theta)\\
&= \mathrm{Tr}[\Theta^{0\prime}\mathcal{W}\mathcal{R}_{\mathcal{S}}^0(\mathcal{R}_{\mathcal{S}}^{0\prime}\mathcal{W}\mathcal{R}_{\mathcal{S}}^0)^{-1}\mathcal{R}_{\mathcal{S}}^{0\prime}\mathcal{W}\Theta^0] \,.
\end{aligned}$$

PROOF OF COROLLARY 1: We need to show that $\Delta_{\mathcal{S}}\mathcal{L}_{\mathcal{S}} \leq \Delta_{\mathcal{S}}\mathcal{L}_{\mathcal{S}} \leq \Delta_{\mathcal{S}}\mathcal{L} + \mathcal{E}_{\mathcal{S}}^0$, where $\Delta_{\mathcal{S}}\mathcal{L}_{\mathcal{S}} = \mathcal{L}^0 - \mathsf{L}(\mathcal{T}_{\mathcal{S}}^*;\phi^0,\theta)$, $\Delta_{\mathcal{S}}\mathcal{L} = \mathcal{L}^0 - \mathsf{L}(\widetilde{\mathcal{T}}_{\mathcal{S}}^*;\phi^0,\theta)$ and $\mathcal{E}_{\mathcal{S}}^0 = \mathcal{L}^0 - \mathrm{Tr}(\Theta_{\mathcal{S}}^{0\prime}\mathcal{W}\Theta_{\mathcal{S}}^0)$. For

the lower bound we note that $\Delta_{\mathcal{S}}\mathcal{L}_{\mathcal{S}} \leq \Delta_{\mathcal{S}}\mathcal{L}$ is implied by $\mathsf{L}(\mathcal{T}^*_{\mathcal{S}};\phi^0,\theta) \geq \mathsf{L}(\widetilde{\mathcal{T}}^*_{\mathcal{S}};\phi^0,\theta)$. For the upper bound $\Delta_{\mathcal{S}}\mathcal{L} \leq \Delta_{\mathcal{S}}\mathcal{L}_{\mathcal{S}} + \mathcal{E}^0_{\mathcal{S}}$ note that

$$\begin{aligned}
\Delta_{\mathcal{S}}\mathcal{L} &= \mathrm{Tr}[\Theta^{0'}\mathcal{W}\mathcal{R}^0_{\mathcal{S}}(\mathcal{R}^{0'}_{\mathcal{S}}\mathcal{W}\mathcal{R}^0_{\mathcal{S}})^{-1}\mathcal{R}^{0'}_{\mathcal{S}}\mathcal{W}\Theta^0] \\
&= \mathrm{Tr}[\Theta^{0'}_{\mathcal{S}}\mathcal{W}\mathcal{R}^0_{\mathcal{S}}(\mathcal{R}^{0'}_{\mathcal{S}}\mathcal{W}\mathcal{R}^0_{\mathcal{S}})^{-1}\mathcal{R}^{0'}_{\mathcal{S}}\mathcal{W}\Theta^0_{\mathcal{S}}] + \mathrm{Tr}[\Theta^{0'}_{-\mathcal{S}}\mathcal{W}\mathcal{R}^0_{\mathcal{S}}(\mathcal{R}^{0'}_{\mathcal{S}}\mathcal{W}\mathcal{R}^0_{\mathcal{S}})^{-1}\mathcal{R}^{0'}_{\mathcal{S}}\mathcal{W}\Theta^0_{-\mathcal{S}}] \\
&\leq \mathrm{Tr}[\Theta^{0'}_{\mathcal{S}}\mathcal{W}\mathcal{R}^0_{\mathcal{S}}(\mathcal{R}^{0'}_{\mathcal{S}}\mathcal{W}\mathcal{R}^0_{\mathcal{S}})^{-1}\mathcal{R}^{0'}_{\mathcal{S}}\mathcal{W}\Theta^0_{\mathcal{S}}] + \mathrm{Tr}[\Theta^{0'}_{-\mathcal{S}}\mathcal{W}\Theta^0_{-\mathcal{S}}] \\
&= \mathrm{Tr}[\Theta^{0'}_{\mathcal{S}}\mathcal{W}\mathcal{R}^0_{\mathcal{S}}(\mathcal{R}^{0'}_{\mathcal{S}}\mathcal{W}\mathcal{R}^0_{\mathcal{S}})^{-1}\mathcal{R}^{0'}_{\mathcal{S}}\mathcal{W}\Theta^0_{\mathcal{S}}] + \mathrm{Tr}[\Theta^{0'}\mathcal{W}\Theta^0] - \mathrm{Tr}[\Theta^{0'}_{\mathcal{S}}\mathcal{W}\Theta^0_{\mathcal{S}}] \\
&= \Delta_{\mathcal{S}}\mathcal{L}_{\mathcal{S}} + \mathcal{E}^0_{\mathcal{S}} \,.
\end{aligned}$$

Q.E.D.

PROOF OF COROLLARY 2: Let $\mathbf{Y}^0 = \Theta^0\mathbf{S}$ be the outcome under ϕ^0 for a given realization of $\mathbf{S}$. Note that $\Sigma^0_Y = \mathbb{E}(\mathbf{Y}^0\mathbf{Y}^{0'}) = \Theta^0\Theta^{0'}$. We have

$$\Delta_{\mathcal{S}}\mathcal{L} = \mathrm{Tr}[\mathcal{W}\mathcal{R}^0_{\mathcal{S}}(\mathcal{R}^{0'}_{\mathcal{S}}\mathcal{W}\mathcal{R}^0_{\mathcal{S}})^{-1}\mathcal{R}^{0'}_{\mathcal{S}}\mathcal{W}\Theta^0\Theta^{0'}] = \mathrm{Tr}[\mathcal{W}\mathcal{R}^0_{\mathcal{S}}(\mathcal{R}^{0'}_{\mathcal{S}}\mathcal{W}\mathcal{R}^0_{\mathcal{S}})^{-1}\mathcal{R}^{0'}_{\mathcal{S}}\mathcal{W}\Sigma^0_Y] \,.$$

Now importantly, $\Sigma^0_Y = \mathbb{E}(\mathbf{Y}^0\mathbf{Y}^{0'})$ is the variance of the outcomes in a timeless problem, i.e. given only $\mathbf{S} = (\boldsymbol{\Xi}', \boldsymbol{\epsilon}')'$ and there are no initial conditions. To compute this variance in practice we need to remove any initial conditions, i.e. for a given point in time we define $\mathbf{U}^0_t = \mathbb{E}_t\mathbf{Y}^0_t - \mathbb{E}_{t-1}\mathbf{Y}^0_t$, where $\mathbb{E}_t(\cdot) = \mathbb{E}(\cdot|\mathcal{F}_t)$ with $\mathcal{F}_t$ the information set that includes all structural shocks up to time t. The innovation $\mathbf{U}^0_t$ then exactly captures the shocks released at time t and the variance $\Sigma^0_U = \mathbb{E}(\mathbf{U}^0_t\mathbf{U}^{0'}_t) = \Sigma_Y$. The final expression follows by using $\Sigma^0_U = \Psi^0\Psi^{0'}$. *Q.E.D.*

PROOF OF COROLLARY 3: Since $\Sigma^0_U = \mathbf{D}\Sigma^c_U\mathbf{D}' + \Sigma^{-c}_U$ by construction, the result follows directly by substitution from Corollary 2

Q.E.D.

S2. ADDITIONAL EMPIRICAL RESULTS

In this section, we present additional empirical results, which complement and extend our main analysis: (i) we report the optimal reaction adjustment (ORA) statistics and all estimated impulse response underlying our policy evaluation statistics (DML and policy path response adjustment statistics), (ii) we assess the statistical significance of changes in policy performances across periods, and (iii) we present counter-factual scenarios to capture how improved policy performance would have affected the historical paths of unemployment and inflation.

S2.1. *Optimal reaction adjustment statistics and impulse responses estimates*

Table S1 reports our baseline optimal reaction adjustment (ORA) estimates underlying the results in Table 1 in the main text.

The impulse responses underlying our policy evaluation statistics (Tables S1 and I) are displayed in Figures S6–S21. The top row shows the impulse responses of inflation, unemployment and the interest rate to a monetary policy shock, while the bottom rows show the responses of the same variables to a non-policy shock.

The ORA adjusted impulse responses (dashed green lines) then show how optimally adjusting the reaction coefficient to financial shocks would have changed the impulse responses of

TABLE S1

EVALUATION US MONETARY POLICY: 1879-2019 — OPTIMAL REACTION ADJUSTMENT (ORA, τ^*)

	Average |ORA|	Categories					
		Bank panics	G	Energy	π^e	TFP	MP
Pre Fed 1879−1912	**0.6**	**−0.9*** (−1.5,−0.3)	**−0.6*** (−1.3,0)	**−0.1** (−0.5,0.4)	—	—	—
Early Fed 1913−1941	**0.5**	**−1.2*** (−1.9,−0.8)	**−0.5*** (−0.9,−0.1)	**0.0** (−0.3,0.3)	**0.7*** (0.3,1.0)	—	—
Post WWII 1951−1984	**0.7**	—	**−0.2** (−0.8,0.3)	**0.8*** (0.1,1.4)	**1.2*** (0.6,1.8)	**0.5** (−0.2,1.2)	—
Post Volcker 1990−2019	**0.2**	**−0.3** (−0.8,0.2)	**0.1** (−0.4,0.6)	**−0.2** (−0.8,0.7)	**−0.1** (−0.4,0.3)	**−0.3** (−0.7,0.1)	—

Note: Median ORA statistics together with 68% credible sets corresponding to different periods and non-policy shocks. The right column ("Average $|ORA|$") reports the average absolute ORAs estimated for each period..

inflation, unemployment and the policy rate. The next section comments on some noteworthy features of these estimated impulse responses.

Responding to financial shocks We already discussed in the main text how, in the Early Fed period, the Fed *raised* the discount rate in response to adverse financial shocks, contrasting with the expansionary policy followed by the Post-Volcker Fed. This finding echoes earlier work on the monetary factors behind the Great Depression (e.g., Friedman and Schwartz, 1963, Hamilton, 1987). But it is also interesting to contrast the Early Fed response with the passive Gold Standard, comparing Figures S10 and S11. In contrast to the Early Fed's contractionary response to financial crises, the interest rate response to financial shocks is mostly negative (i.e., expansionary) during the Pre Fed period. In other words, the Early Fed's response to financial shocks is more contractionary (and thus worse) than during the gold standard.

In the early Fed period, the optimal reaction adjustment ($\tau^* = -1.2$) would have transformed the contractionary policy response into an expansionary one. In contrast, in the post Volcker period, the ORA ($\tau^* = -0.3$) moderately lowers the response of the policy rate, leading to modest effects on the responses of inflation and unemployment.

Responding to energy and TFP shocks For the post WWII period, we also estimated large ORAs in response to energy shocks and TFP shocks. To understand the determinants of these ORA estimates, Figures S15 and S20 plot the underlying impulse responses estimated over the post WWII period. The impulse responses to monetary shocks are in line with earlier evidence (e.g., Coibion, 2012). In response to an energy price shock or an inflation expectation shock, inflation rises progressively, while the policy rate response is relatively mild. In fact, in both cases the real interest rate declines following an energy price shock or adverse TFP shock. In other words, the Taylor principle is not satisfied, a finding echoing an earlier literature on the performance of the Fed during the 1970s (Clarida et al., 2000, Leduc et al., 2007). However, we can go further and compute how the policy rate should have responded to these shocks, as displayed by the dashed green lines. The adjustment restores the Taylor principle and the real rate rises following both shocks.

It is interesting to contrast these sub-optimal reactions with the "appropriate" reactions of the post Volcker period. Figures S16 and S21 plot the impulse responses to energy price shocks and TFP shocks estimated over the Post Volcker period. In response to an energy price shock, the inflation response is short-lived, too fast for monetary policy to have a chance at preventing the transitory inflationary burst. With the impulse responses to policy and non-policy shocks close to orthogonal, the ORA is small and non-significant: the reaction function can be considered

appropriate. Similarly, in response to an adverse TFP shock the inflation increase is moderate and transitory, and the ORA is again non-significant. In other words, we cannot reject that Greenspan's reaction to the IT productivity gains was appropriate, thereby confirming previous narrative accounts in the literature (e.g., Blinder and Reis, 2005).[1]

Importantly, note that the non-significance of all our Post Volcker ORA estimates is *not* due to imprecisely estimated impulse responses. In all cases, the impulse responses are estimated with reasonable precisions, and the point estimates are sensible, meaning that the ORAs are small, *because* the impulse responses to non-policy shocks are (almost) orthogonal to the impulse responses to policy shocks.

Responding to government spending shocks While monetary studies of the early Fed have focused on the monetary response to financial distress, our approach allows to study and compare performance in response to other prominent shocks. Figures S7 plots the impulse responses to negative government spending shocks in the Early Fed period. We can see that the Fed's failure to react to adverse financial shocks extends to adverse government spending shocks. In fact, similarly to the overly contractionary response to adverse financial shocks, the Fed was also running a contractionary policy following adverse spending shocks, thereby amplifying the negative unemployment effects of the shocks (green line, lower right panel).

S2.2. *Posterior probabilities of reaction function improvements*

To get a sense of the statistical significance of the changes of policy performance over time —improvements in the Fed's reaction function—, Table S2 reports the posterior probabilities for $P\left(\frac{\text{avg}(\Delta_S \Theta^{\text{B}}_{p,s})}{|\text{avg}(\Theta^{\text{B}}_{p,s})|} < \frac{\text{avg}(\Delta_S \Theta^{\text{A}}_{p,s})}{|\text{avg}(\Theta^{\text{A}}_{p,s})|}\right)$, the percentage correction to the policy path response for each shock type s. This "'percentage correction" is a unitless summary measure that conveys how far off was the Fed to best responding to a particular shock type that it faced.

A large posterior probability indicates a large probability that the Fed improved its reaction function in period B compared to period A when faced with shock category s. Conversely, a low value indicates a large probability that the reaction function worsened in period B compared to period A.

The main results of the paper can be seen in that table. First, the post Volcker stands out with large posterior probabilities that the reaction function improved relative to the Early Fed or the Post WWII Fed. For instance, for financial shocks there is an 87 percent probability that the percentage reaction adjustment is smaller for the Post Volcker Fed than for the Early Fed. Similarly, for inflation expectation shocks, there is a 90 percent probability that the percentage reaction adjustment is smaller for the Post Volcker Fed than for the Post WWII Fed. More generally, for the Post Volcker posterior probabilities of reaction function improvements are above 68 percent (see "Post Volcker" rows) for most shocks and most periods.

Another interesting finding is the worse performance of the Early Fed relative to the Gold Standard, and the posterior probabilities confirm the significance of this result with a 68 percent (1-0.32) posterior probability that the Early Fed reacted worse than the passive Gold Standard to financial shocks (see the first entry at 0.32 in the "Bank panics" panel). Similarly, for energy shocks there is a 72 percent posterior probability (1-0.28=0.72) that the Early Fed had a worse

[1] That said, the ORA is negative at -0.3, and in response to the positive TFP shocks identified in the late 90s, the ORA calls for slightly higher fed funds rate than pursued by Greenspan at the time (see Figures S4 and S5). The point estimate suggests that monetary policy may have been slightly too accommodative (by about 0.25 ppt), though again the estimate is non-significant.

reaction function than the passive Gold Standard. For government spending shocks, the evidence is less strong with "only" 57 percent posterior probability (1-0.43=0.57) that the Early Fed did worse.

Last, we can notice the relatively strong evidence that the policy response to supply-type shocks (notably inflation expectation shocks) deteriorated in the Post WWII regime relative to the Early Fed with a posterior probability of worse reaction of 78 percent (1-0.22=0.78).

TABLE S2
POSTERIOR PROBABILITIES $P\left(\|\Delta\Theta^{\text{B}}_{p,s}\|/\|\Theta^{\text{B}}_{p,s}\| < \|\Delta\Theta^{\text{A}}_{p,s}\|/\|\Theta^{\text{A}}_{p,s}\|\right)$

	Bank panics	Pre Fed	Early Fed	A Post WWII	Post Volcker
B	Pre Fed	—			
	Early Fed	0.32	—		
	Post WWII	—	—	—	
	Post Volcker	0.68	0.87	—	—
	G	Pre Fed	Early Fed	A Post WWII	Post Volcker
B	Pre Fed	—			
	Early Fed	0.43	—		
	Post WWII	0.54	0.58	—	
	Post Volcker	0.76	0.79	0.62	—
	Energy	Pre Fed	Early Fed	A Post WWII	Post Volcker
B	Pre Fed	—			
	Early Fed	0.28	—		
	Post WWII	0.21	0.43	—	
	Post Volcker	0.50	0.64	0.67	—
	$\boldsymbol{\pi^e}$	Pre Fed	Early Fed	A Post WWII	Post Volcker
B	Pre Fed	—			
	Early Fed	—	—		
	Post WWII	—	0.22	—	
	Post Volcker	—	0.81	0.90	—

Note: The table reports the posterior probabilities that the percentage policy response correction is smaller in period B relative to period A. Each panel refers to the policy response correction for a specific shock category: financial shocks ("bank panics"), government spending shocks ("G"), energy price shocks ("Energy") and inflation expectation shocks ("π^e").

S2.3. *Counterfactual historical policy scenarios*

Our sufficient statistics approach also allows to create counter-factual historical policy paths. Specifically, one can quantify and visualize how much variations in inflation and unemployment could have been avoided if the Fed had use a (subset) optimal reaction to the specific macro shocks we identified.

Specifically, given the identified non-policy shocks $\mathbf{S}_{\mathcal{S}} = (\boldsymbol{\epsilon}_{\mathcal{S}}, \Xi_{\mathcal{S}})$, Lemma 2 implies

$$\mathbf{Y} = \mathbf{Y}^0 + \mathcal{R}^0_{\mathcal{S}}\mathcal{T}^*_{\mathcal{S}}\mathbf{S}_{\mathcal{S}} \qquad \text{and} \qquad \mathbf{P} = \mathbf{P}^0 + \mathcal{R}^0_{p,\mathcal{S}}\mathcal{T}^*_{\mathcal{S}}\mathbf{S}_{\mathcal{S}} \tag{S5}$$

We can then implement these counter-factual calculations for shocks realizations $\mathbf{S}_{\mathcal{S},t}$ for any sample $t = t_s, \ldots, t_e$.

Figure S4 plots the counter-factual paths for the policy rate, inflation and unemployment. These counter-factuals convey how our estimated ORA policy rule adjustments would have translated into different paths for the policy rate, inflation and unemployment. In particular the "ORA-adjusted terms" (red lines) capture the variation in inflation and unemployment that could have been avoided with a different reaction function. In addition, to help isolate the contributions of the different non-policy shocks to these ORA adjustments, Figure S5 decomposes the ORA adjustments to the policy rate into the contributions of the different macro shocks; allowing to isolate the shocks responsible for the largest "welfare" losses.

In the pre Fed period, there were substantial deviations from an optimal reaction coefficients, calling for lower interest rates (about 3/4 ppt) in the aftermaths of the 1893 and 1907 bank runs, as well as higher interest rates in response to higher military spending following the war against Spain in 1898, and the navy build-up of 1902-1904 (Figure S5, left column). That said, over the pre Fed period, our identified macro shocks explain only a small share of the total variance of inflation and unemployment over 1879-1912, so that the ORA adjustments only have a moderate effect on the variance of inflation and unemployment over that period.

In the early Fed period, the ORAs translate into large adjustments to the discount rate. First, the large increase in military spending over 1918 is responsible for part of the inflation outburst in 1919-1920, and the ORA calls for an almost 1ppt higher discount rate to tame that increase. Second, and most strikingly, the ORA calls for large adjustments in the early stage of the Great Depression (1931-1932). In response to the bank runs and the negative inflation expectation shocks of 1931-1932 (Figure S5), the ORA cancels the discount rate increases observed in 1931 —hikes that have been criticized for turning the initial late 1929 recession into a full blown depression (e.g., Hamilton, 1987)— and lowers the discount rate all the way to almost (but still above) zero in 1932. This would have avoided 8 percentage points in unemployment and it would have also avoided the ensuing deflation. The re-inflation shock following Roosevelt's election would have then been countered by a higher discount rate.[2]

Turning to the post world war II period, the ORA calls for substantially higher fed funds rate throughout the 1960-1980 period. While the ORA does call for more tightening (about 1/2 ppt) in the face of large government programs related to US space program in the early 60s and the Vietnam war in the second half of the 60s, the largest adjustments by far occur during the 70s (as much as 6 ppt higher fed funds rate) in response to the oil price shocks of 1974 and 1979 and the inflation expectation shocks occurring during that period. With such strong response, as much as about 5 ppt of inflation could have been avoided (at the cost of extra unemployment), see Figure S4. In fact, one might argue that the higher "trend" inflation of the 1970s could have been avoided.

In contrast, for the post Volcker period the policy rate adjustments are small except in the early phase of the Great Recession with the ORA calling for an additional 0.5 ppt drop in the fed funds rate in 2009, something not possible because of the zero lower bound. Interestingly, this case contrasts with the Great Depression where the discount rate is not constrained by the ZLB *even* after the ORA adjustment. While the ORA calls for a whole 2 ppt lower discount rate in 1931-1932, this would have left the discount rate above zero. Unlike in the Great Recession, we can thus attribute all of the ORA correction to the sub-optimal reaction function of the early Fed.

[2]Of course, had the US avoided the deflation and the large unemployment run-up, such a re-inflation shock would not have happened, for instance because Roosevelt may not even have been elected. This counter-factual exercise is based on an ex-post realization of shocks.

S3. ROBUSTNESS CHECKS

In this section, we report the results to two robustness checks: (i) expanding the set of identified monetary shocks in the Post WWII and the Post Volcker periods, (ii) robustness to alternative definitions of the monetary regimes. Additional robustness checks are presented in the Supplementary Material.

In the interest of space, we will report the robustness results for the ORA estimates only, as the ORA underlies the distance to minimum loss and optimal adjustment to the policy path response.

S3.1. *Expanding $\mathcal{S}$-subset policy evaluation*

The baseline results are based on using one monetary shock to evaluate policy makers reaction functions. One concern when comparing policy makers across different regimes is that the identifying monetary shocks are different across regime. Intuitively, if the policy experiment has a different dynamic composition across regimes, one could be evaluating policy makers in "different directions" of policy performance.

We saw in the main text that the policy path responses to policy shocks were very similar across the first three periods —capturing a short-run change in the policy rate—, but slightly more protracted in the final period, the post-Volcker Fed. As robustness check, we thus focus on the two recent periods (Post-WWII and Post-Volcker), and we exploit recent progress in the literature in order to isolate multiple policy shocks and span a richer set of dynamic perturbations.

For the Post WWII period, our baseline Romer and Romer (2004b) shocks capture only short-lived changes to the policy path. To capture more persistent changes, we exploit the recent work of Romer and Romer (2024) and use as our second policy shock series the Romer and Romer (2024)'s series of policy shocks with high degree of dis-inflation commitment. More precisely, we start from the dis-inflationary monetary shocks of Romer and Romer (1989), which capture "times when Federal Reserve policymakers decided that the current inflation rate was unacceptable (with output at potential), and took contractionary actions to reduce it", and we exploit Romer and Romer (2024)'s recent insight that these different dis-inflationary episodes varied in their degree of commitment. Indeed, after analyzing the records of policy discussions Romer and Romer (2024) discovered important differences in policymakers' degree of commitment to disinflation at the times the policies were embarked on. By focusing on the dis-inflationary episodes with the highest degree of commitment, we can hope to isolate more persistent policy changes.

We estimate a Bayesian VAR as in the baseline setup except that we have two monetary shocks, ordering the high-commitment dis-inflationary shock before the Romer and Romer (2004b) shock used in our baseline results. The top panel of Figure S1 plots the estimated IR of FFR following a Romer and Romer (2024) dis-inflation shock with high degree of commitment, while the middle panel plots the IR estimated in response to a Romer and Romer (2004b) shock. Confirming our conjecture, highly credible dis-inflationary episodes engineer a persistent increase in the fed funds rate. In contrast, the policy experiment associated with the Romer and Romer (2004b) shocks are much more short lived. Combining these two monetary shocks will thus permit a more exhaustive assessment of policy makers' reaction function in the Post WWII regime.

For the Post-Volcker regime, we exploit again the high-frequency based identification allowed by futures market, following Kuttner (2001), Eberly et al. (2020). For the first shock, we use surprises to the fed funds rate —the difference between the expected fed funds rate (as implied by three-month federal funds futures contracts, FF4) and the actual fed funds rate—,

FIGURE S1.—Post WWII Fed, Two-shocks evaluation, Reaction to π^e shock

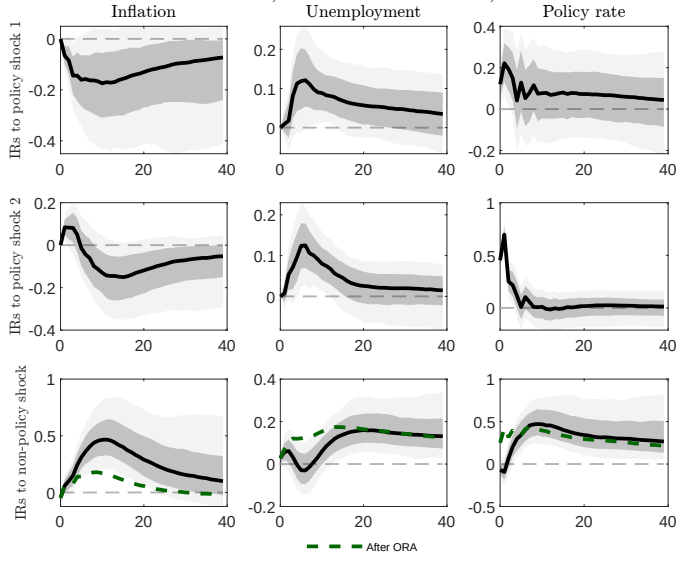

FIGURE S2.—Post Volcker Fed, Two-shocks evaluation, Reaction to financial shock

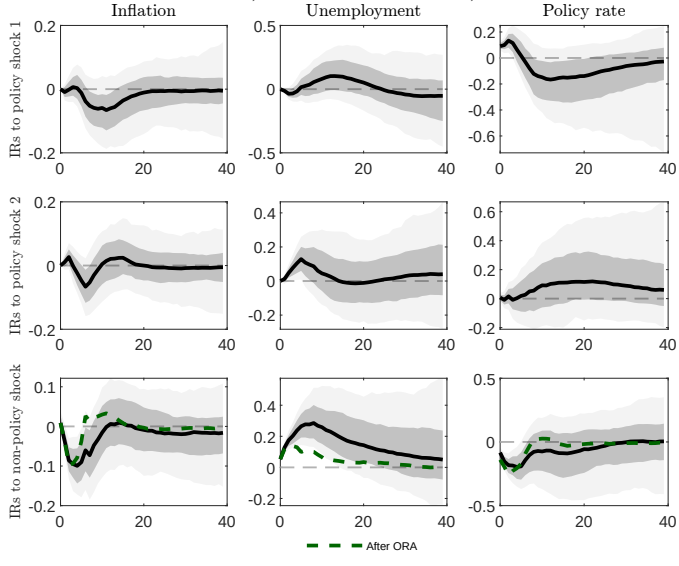

Note: Shaded areas depict the 68% credible sets.

and for the second shock we use surprises to the two-year on-the-run Treasury yield (OR2), orthogonalized with respect to surprises to the current fed funds rate, to identify the effects of shocks to the medium end of the yield curve. The top row of Figure S2 plots the estimated impulse responses following a surprise to the 3-month fed funds future (FF4), while the middle row plots the impulse responses to a surprise to the 2-year on-the-run treasury yield. We can see that the OR2 surprise allows us to isolate more persistent increase in the fed funds rate. In contrast, the policy experiment associated with the FF4 surprise is more short lived. Combining

these two monetary shocks will thus permit a more exhaustive assessment of policy makers' reaction function in the Post–Volcker regime.

Table S3 reports the subset DMLs and policy path response adjustment as estimated from this larger subset of policy shocks $\mathcal{S}_p$. First, note that the DMLs are slightly larger than in the baseline estimates. This is to be expected as we are now considering a broader range of policy experiments. Nonetheless, we have a similar ratio of DML between the two periods, with the post-Volcker regime achieving about half of the distance to minimum loss as the Pre-Volcker regime: 5.9 vs 9.5.

TABLE S3

ROBUSTNESS: EVALUATION WITH TWO MONETARY SHOCKS

Panel (i) Distances to Minimum Loss (DML)

	Overall	By shock category					
		Bank panics	G	Energy	π^e	TFP	MP
Post WWII 1951−1984	**9.5** (5.5,18.4)	—	**0.3** (0.1,1.1)	**1** (0.2,4.2)	**1.9** (0.5,5.9)	**0.7** (0.1,3.2)	**2.1** (1.2,3.9)
Post Volcker 1990−2019	**5.9** (3,14.7)	**0.9** (0.3,3.1)	**0.5** (0.1,2.1)	**0.5** (0.1,1.8)	**0.2** (0,1)	**0.5** (0.1,2)	**1.4** (0.6,3.4)

Panel (ii) Distance to optimal policy path response ($\frac{\|\Delta\Theta_{p,s}\|}{\|\Theta_{p,s}\|}$)

	By shock category					
	Bank panics	G	Energy	π^e	TFP	MP
Post WWII 1951−1984	—	**−1.5** (−5.6,0.9)	**0.4** (−0.3,1.3)	**4.3*** (0.4,16.4)	**0.5** (−2.4,3.7)	—
Post Volcker 1990−2019	**−0.4** (−1.3,0.3)	**−0.2** (−1.7,1.3)	**0.1** (−5.5,6.4)	**−0.3** (−3.1,2.9)	**−1.2** (−6.5,1.6)	—

Note: Panel (i) shows the median subset distance to minimum loss; overall ($\Delta_{\mathcal{S}_p}\mathcal{L}$, first column) and shock-specific ($\Delta_{\mathcal{S}_p}\mathcal{L}_s$) together with 68% credible sets in parentheses with each row reporting estimates for a different period. In the first column, the brackets report median estimates for the upper and lower bounds for $\Delta_{\mathcal{S}_p}\mathcal{L}$. Panel (ii) shows the median percentage correction to the policy path reaction to each identified macro shock with 68% credible sets in parentheses. See main text for shocks definition and identification.

Overall, the policy path response adjustments obtained with two monetary shocks are very similar to our conclusions obtained with only one monetary shock. This indicates that the room for improvement was mostly on the short-end of the policy path.

S3.2. *Alternative monetary periods*

We consider robustness to the definition of the monetary period. Table S4 display ORA estimated for alternative definition of the monetary regime: (i) the Gold Standard period over 1879-1932,[3], (ii) the interwar period after the US went off the Gold Standard in 1933, (iii) the Bretton Woods system (1946-1971), (iv) the post Bretton Woods period until the beginning of the Great Moderation (1971-1984), and (v) a pre Volcker period (1951-1979).

[3]In the baseline specification, we treated the Early Fed period as different from the Gold Standard, as the Fed had considerably leeway in varying its god cover ratio. That said, the extent to which the Gold Standard limited Fed monetary policy remains a debated question (e.g., Eichengreen, 1992, Hsieh and Romer, 2006).

Overall the results confirm our main finding with no uniform improvements in performance until 1984, poor (i.e., too passive) reaction to bank panics during the Gold Standard (passive or active) period, and similarly poor (i.e., too passive) reaction to supply-side shocks in the post WWII period. We also note an interesting and novel result: the ORA for government spending is significantly negative for the Bretton Woods period (1946-1971). Since the government spending shocks of the 1960s were mostly positive (capturing two large government programs related to US space program in the early 60s and the Vietnam war in the second half of the 60s), our estimated ORA implies that the Fed did not raise the policy rate enough in the face of these large government programs, confirming earlier narrative evidence of a too soft reaction of William Martin's Fed during that period Romer and Romer (2004a), Hack et al. (2023).

TABLE S4

ORA STATISTICS, ALTERNATIVE REGIME DEFINITION

Non-policy shock Shock sign convention	Bank panics $u \uparrow$	G $u \uparrow$	Energy $\pi \uparrow$	π^e $\pi \uparrow$	TFP $\pi \uparrow$
Gold Standard 1879−1932	$\mathbf{-0.9}^*$ $(-1.2,-0.6)$	$\mathbf{-0.3}^*$ $(-0.6,-0.1)$	$\mathbf{-0.1}$ $(-0.4,0.2)$	$\mathbf{0.8}$ $(-0.8,1.6)$	—
Interwar, off Gold 1933−1941	—	$\mathbf{-1.1}$ $(-3.7,3.3)$	$\mathbf{-0.1}$ $(-0.9,0.7)$	$\mathbf{0.3}$ $(-0.4,1)$	—
Bretton Woods 1946−1971	—	$\mathbf{-0.6}^*$ $(-0.9,-0.2)$	$\mathbf{-0.2}$ $(-0.8,0.4)$	$\mathbf{0.3}$ $(-0.3,0.8)$	$\mathbf{0.4}$ $(-0.1,0.8)$
Post Bretton Woods 1971−1984	—	$\mathbf{0.0}$ $(-0.5,0.6)$	$\mathbf{0.7}$ $(-0.2,1.3)$	$\mathbf{0.8}^*$ $(0.0,1.2)$	$\mathbf{0.6}$ $(-0.1,1.2)$
Pre Volcker 1951−1979	—	$\mathbf{-0.4}^*$ $(-0.7,0.0)$	$\mathbf{0.2}$ $(-0.4,0.7)$	$\mathbf{0.6}^*$ $(0.0,1.0)$	$\mathbf{0.3}$ $(-0.2,0.9)$

Note: Median ORA statistics together with 68% credible sets. See the main text for shock identification assumptions.

Last, this robustness exercise also highlights a trade-off inherent to our sufficient statistics approach. Our method requires large enough samples and/or samples with sufficiently large shocks in order to estimate the impulse responses with enough confidence. The interwar period for instance is a very short sample, and all the ORAs are consequently estimated with large error bands. This does not invalidate the approach, but it makes it inference more difficult. Similarly for the Bretton Woods period; there were no major energy price shocks during that period, making the ORA uncertain.

S4. LARGE GOLD DISCOVERIES AND EXTRACTION MAXIMA

In this section, we describe how we constructed our instrumental variable for movements in the monetary base under the passive Gold Standard of 1879-1912.

Under a Gold Standard, the monetary base depends on the amount of gold in circulation, which can itself vary for exogenous reasons related to the random nature of gold discoveries or development of new extraction techniques (e.g., Barsky and De Long, 1991). As such, we use large gold mine discoveries (the dates of discoveries that led to gold rushes) and mine peak

extraction (the dates when these large mines reached peak production) to create an instrument variable for movements in the monetary base. Given the historical difficulty in predicting the amount of gold available in any given region (either at the onset of a gold rush or at its zenith), we can consider these events as unanticipated and unrelated to the state of the business cycle.

To inform our narrative identification, we rely on Koschmann and Bergendahl (1968), which is a detailed account of Gold production districts in the US since 1799. See the Supplementary Material where Figures S22–S25 show gold production in four states that experienced large gold rushes. In each case, the gold rush led to large variations in gold production; in the order of 30-40 percent of *national* production.

Figure S3 plots national gold production along with our identified dates for the discoveries of large mines. We also report peak extraction dates when the date could be unambiguously identified from the narrative accounts. The large discovery and peak extraction dates are the Sutter's Mill discovery in California, the Comstock lode mine discovery in Nevada, the Comstock lode maximum (1877-Q1), the Cripple Creek discovery in Colorado (1891-Q3), the Bonanza creek discovery in Alaska (1896-Q3), the Goldfield discovery in Nevada in (1902-Q1), the Goldfield maximum in Nevada (1910-Q1) and the Juneau maximum in Alaska. Since our passive Gold Standard period covers 1879-1912, we only use the dates above that are explicitly spelled in parentheses.

We code the Gold shocks as one when a new mine was discovered and minus one when the peak was reached.

FIGURE S3.— US Gold Production, 1845–1930

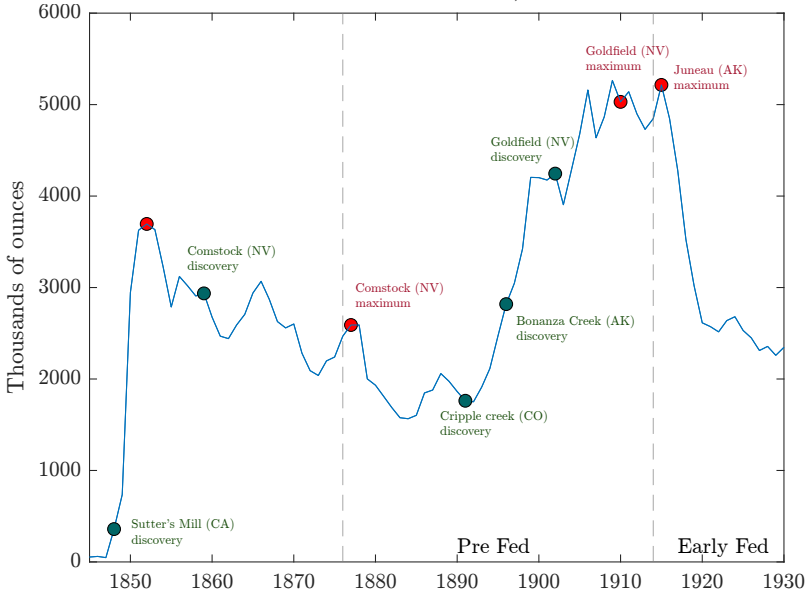

Note: US gold production in thousands of ounces. The green dots correspond to large mine discoveries and the red dots correspond to peak extractions.

BIBLIOGRAPHY

BARSKY, ROBERT B AND J BRADFORD DE LONG (1991): "Forecasting pre-World War I inflation: the Fisher effect and the gold standard," *The Quarterly Journal of Economics*, 106 (3), 815–836. [13]

BLINDER, ALAN S AND RICARDO REIS (2005): "Understanding the Greenspan standard," in *Proceedings-Economic Policy Symposium-Jackson Hole*, Federal Reserve Bank of Kansas City, Aug, 11–96. [7]

CLARIDA, RICHARD, JORDI GALÍ, AND MARK GERTLER (2000): "Monetary Policy Rules and Macroeconomic Stability: Evidence and Some Theory," *The Quarterly Journal of Economics*, 115 (1), 147–180. [6]

COIBION, OLIVIER (2012): "Are the Effects of Monetary Policy Shocks Big or Small?" *American Economic Journal: Macroeconomics*, 4, 1–32. [6]

EBERLY, JANICE C., JAMES H. STOCK, AND JONATHAN H. WRIGHT (2020): "The Federal Reserve's Current Framework for Monetary Policy: A Review and Assessment," *International Journal of Central Banking*, 16 (1), 5–71. [10]

EICHENGREEN, B (1992): "Golden Fetters Oxford: Oxford University Press," . [12]

FRIEDMAN, MILTON AND ANNA JACOBSON SCHWARTZ (1963): *A monetary history of the United States, 1867-1960*, Princeton University Press. [6]

HACK, LUKAS, KLODIANA ISTREFI, AND MATTHIAS MEIER (2023): "Identification of Systematic Monetary Policy," Tech. rep., University of Bonn and University of Mannheim, Germany. [13]

HAMILTON, JAMES D. (1987): "Monetary factors in the great depression," *Journal of Monetary Economics*, 19 (2), 145–169. [6, 9]

HSIEH, CHANG-TAI AND CHRISTINA D ROMER (2006): "Was the Federal Reserve constrained by the gold standard during the Great Depression? Evidence from the 1932 open market purchase program," *The Journal of Economic History*, 66 (1), 140–176. [12]

KOSCHMANN, ALBERT HEINRICH AND MAXIMILIAN H BERGENDAHL (1968): "Principal Gold-Producing Districts of the United States: a description of the geology, mining history, and production of the major gold-mining districts in 21 States," *Professional paper/US Department of the Interior, US Geological Survey*. [14]

KUTTNER, KENNETH N. (2001): "Monetary Policy Surprises and Interest Rates: Evidence from the Fed Funds Futures Market," *Journal of Monetary Economics*, 47 (3), 523–544. [10]

LEDUC, SYLVAIN, KEITH SILL, AND TOM STARK (2007): "Self-fulfilling expectations and the inflation of the 1970s: Evidence from the Livingston Survey," *Journal of Monetary economics*, 54 (2), 433–459. [6]

ROMER, CHRISTINA D AND DAVID H ROMER (1989): "Does monetary policy matter? A new test in the spirit of Friedman and Schwartz," *NBER macroeconomics annual*, 4, 121–170. [10]

——— (2004a): "Choosing the Federal Reserve chair: lessons from history," *Journal of Economic Perspectives*, 18 (1), 129–162. [13]

ROMER, CHRISTINA D. AND DAVID H. ROMER (2004b): "A New Measure of Monetary Shocks: Derivation and Implications," *American Economic Review*, 94, 1055–1084. [10]

ROMER, CHRISTINA D AND DAVID H ROMER (2024): "Lessons from history for successful disinflation," *Journal of Monetary Economics*, 148, 103654. [10]

FIGURE S4.— Counter-factuals under subset-optimal policy, 1879-2019

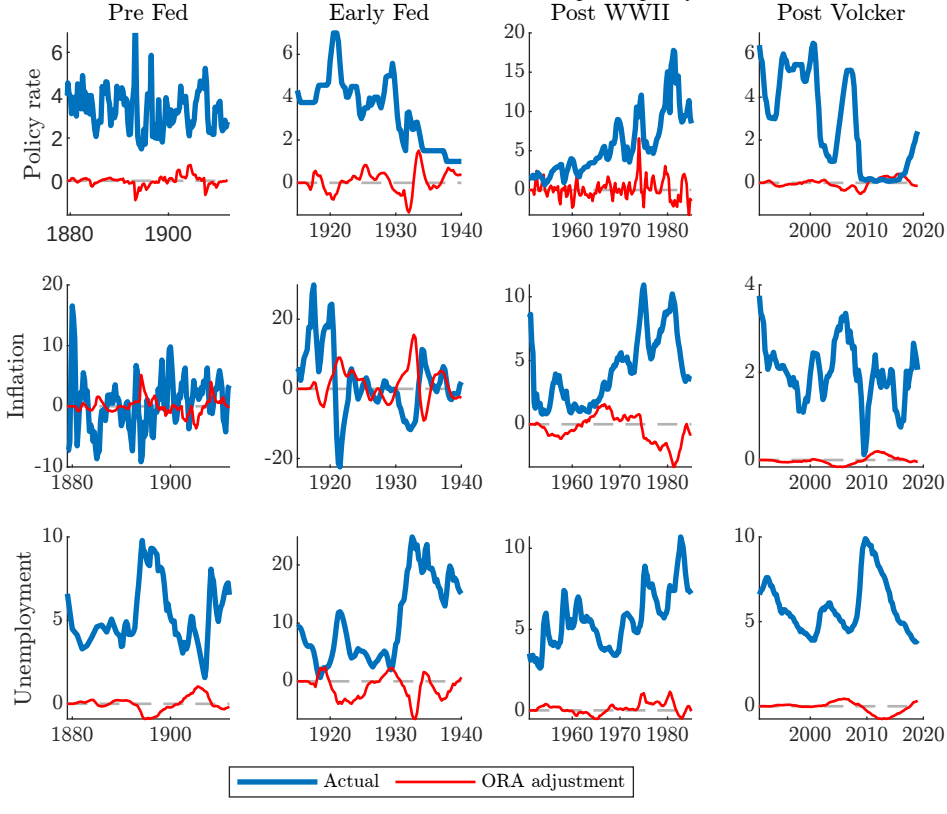

Note: The top row shows the policy rate ("raw data", blue plain line) along with the adjustment to the contemporaneous policy rate implied by the median subset-optimal reaction function adjustment ("ORA adjustment", dashed red line) over each period, calculated following (S5). The middle and bottom rows show the same information but for the inflation rate and the unemployment rate.

FIGURE S5.—Decomposition of the optimal policy rate adjustment, 1879-2019

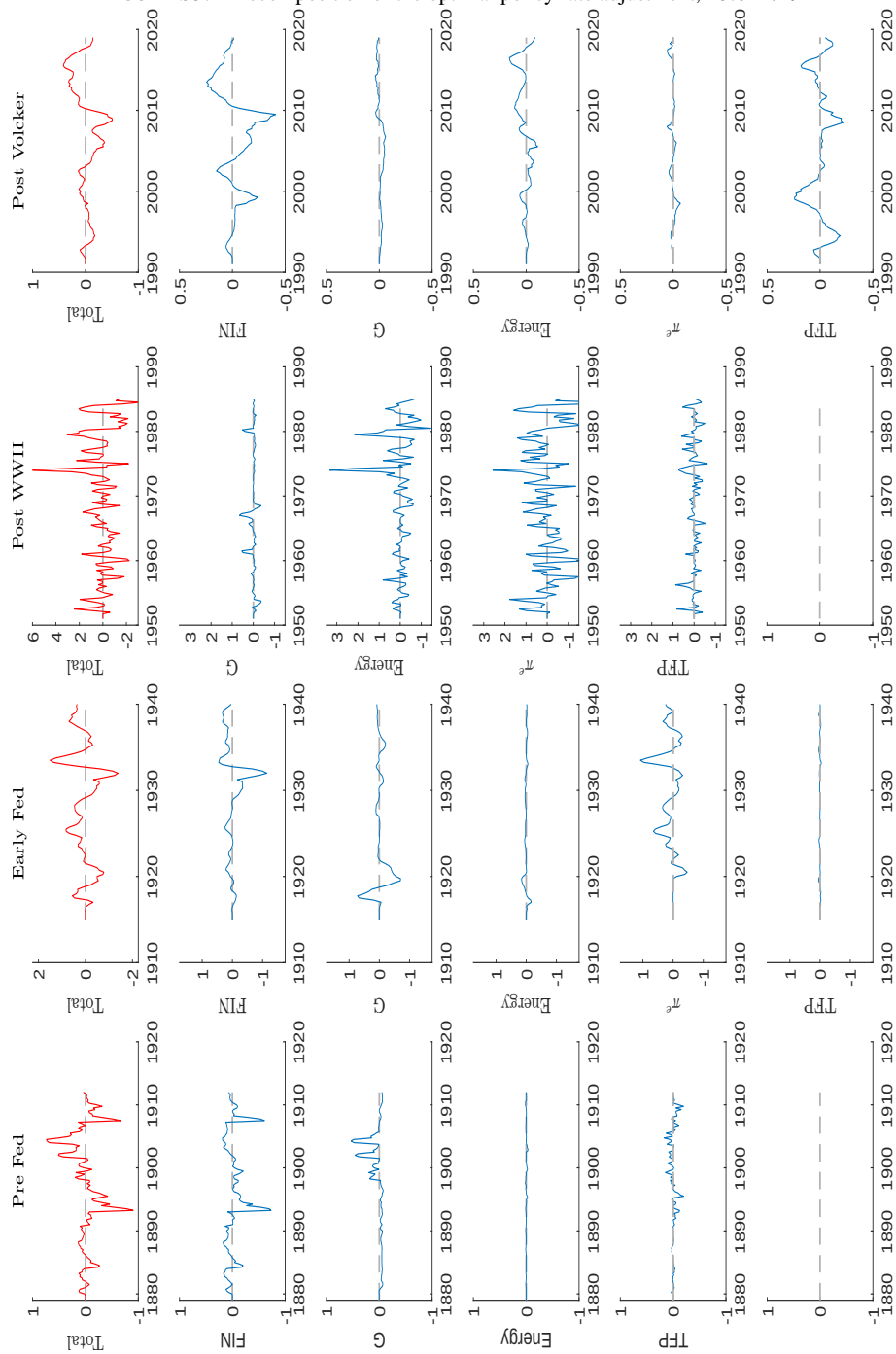

Note: Each column decomposes the (median) optimal adjustment to the contemporaneous policy rate in the contribution of each non-policy shock: financial (FIN), government spending (G), Energy price (Energy), inflation expectations (π^e) and TFP for the four periods: Pre Fed, Early Fed, Post WWII and Post Volcker. The total policy rate adjustment to the contemporaneous policy rate is depicted in the top row.

FIGURE S6.— Pre Fed, 1879-1912, Reaction to G shocks

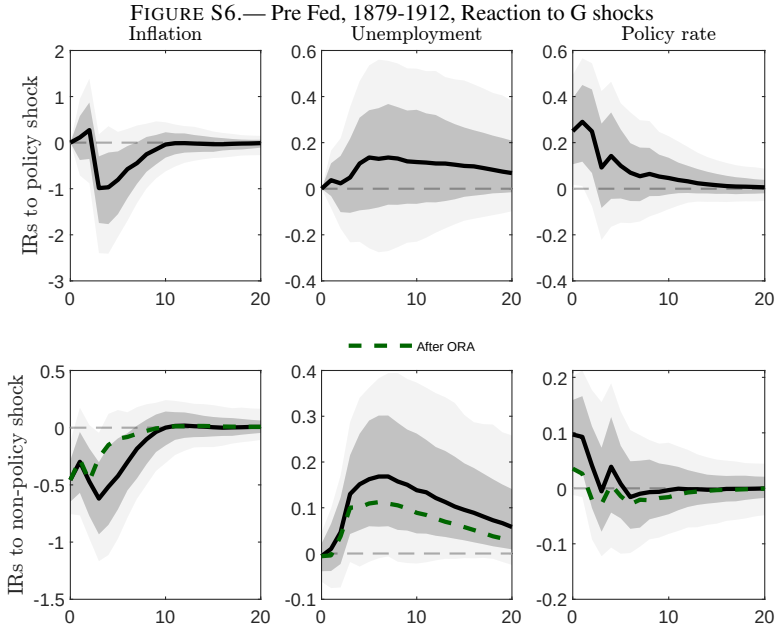

FIGURE S7.— Early Fed, 1913-1941, Reaction to G shocks

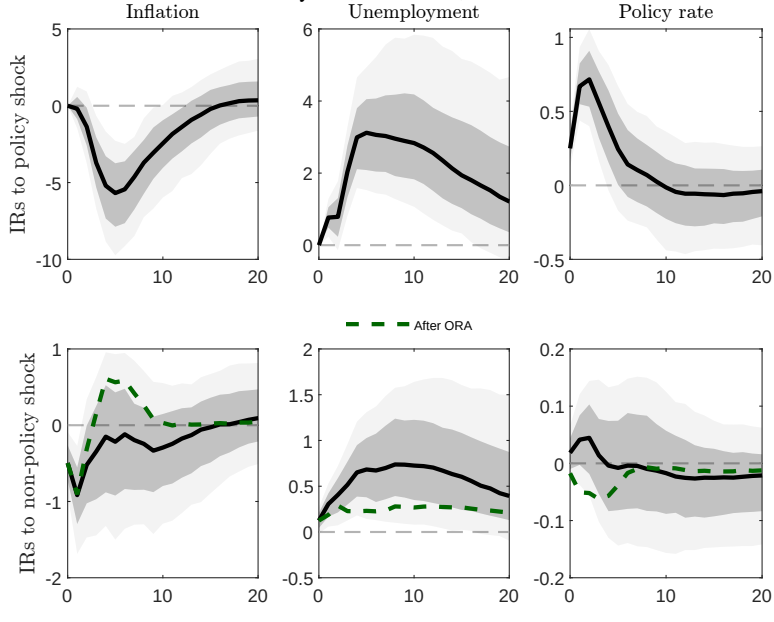

Note: The top row shows the median responses (thick line) of inflation, unemployment and the policy rate to a monetary policy shock. The bottom row shows the median responses (thick line) of inflation, unemployment and the policy rate to a government spending shock. The dotted green lines show the ORA adjusted impulse responses $\Gamma_0^0 + \mathcal{R}_0^0 \tau_0^*$. The 95% and 68% credible sets are plotted as dark and light shaded areas, respectively.

FIGURE S8.— Post WWII Fed, 1951-1984, Reaction to G shocks

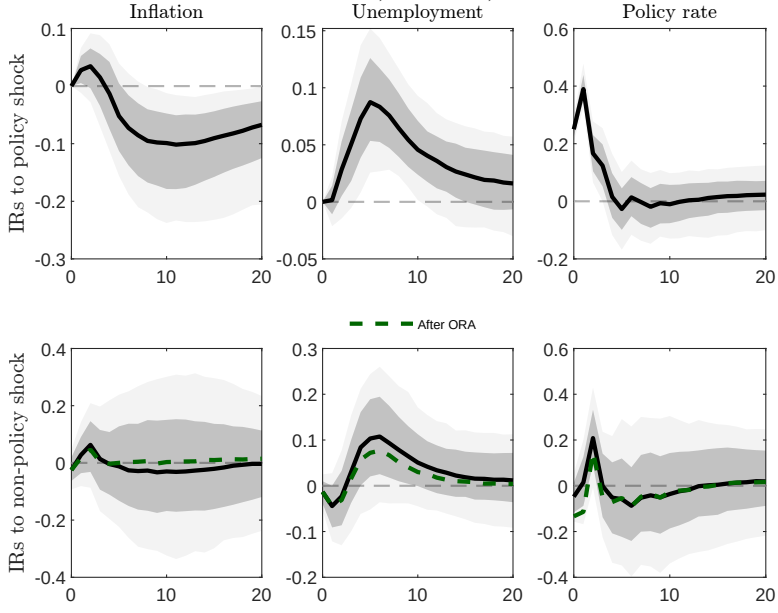

FIGURE S9.— Post Volcker Fed, 1990-2019, Reaction to G shocks

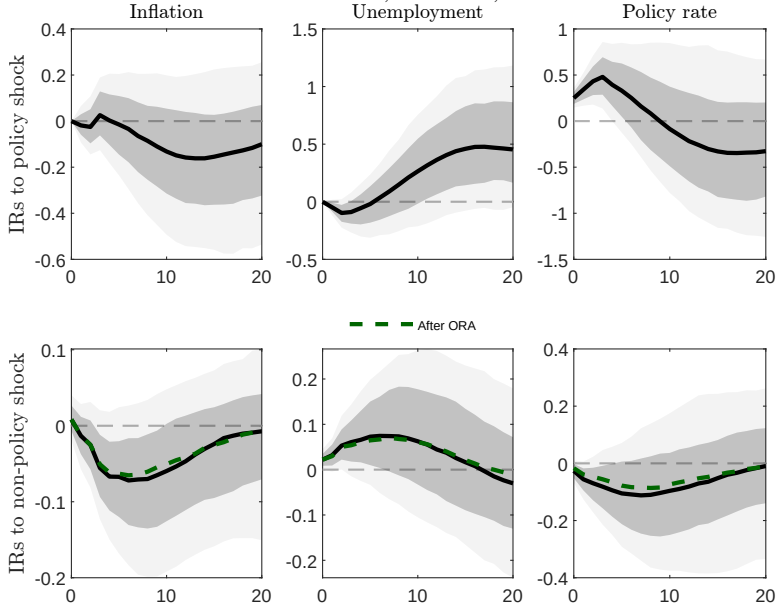

Note: The top row shows the median responses (thick line) of inflation, unemployment and the policy rate to a monetary policy shock. The bottom row shows the median responses (thick line) of inflation, unemployment and the policy rate to a government spending shock. The dotted green lines show the ORA adjusted impulse responses $\Gamma_0^0 + \mathcal{R}_0^0 \tau_0^*$. The 95% and 68% credible sets are plotted as dark and light shaded areas, respectively.

FIGURE S10.— Pre Fed, 1879-1912, Reaction to Financial shocks

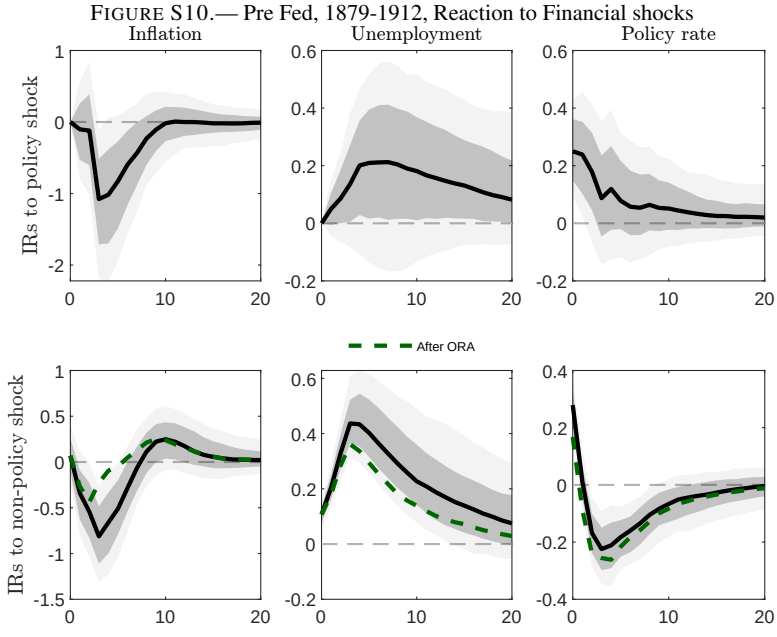

FIGURE S11.— Early Fed, 1913-1941, Reaction to Financial shocks

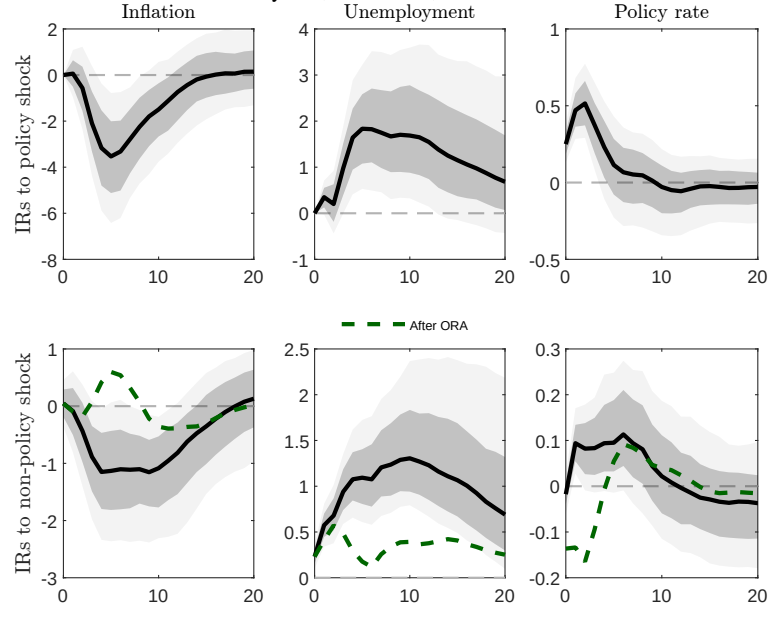

Note: The top row shows the median responses (thick line) of inflation, unemployment and the policy rate to a monetary policy shock. The bottom row shows the median responses (thick line) of inflation, unemployment and the policy rate to a bank panic. The dotted green lines show the ORA adjusted impulse responses $\Gamma_0^0 + \mathcal{R}_0^0 \tau_0^*$. The 95% and 68% credible sets are plotted as dark and light shaded areas, respectively.

FIGURE S12.— Post Volcker Fed, 1990-2019, Reaction to Financial shocks

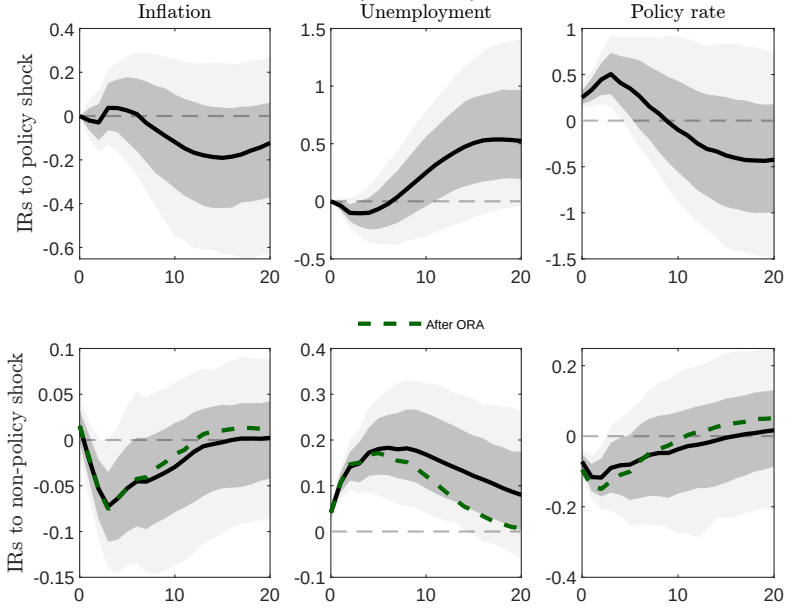

FIGURE S13.— Pre Fed, 1879-1912, Reaction to Energy shocks

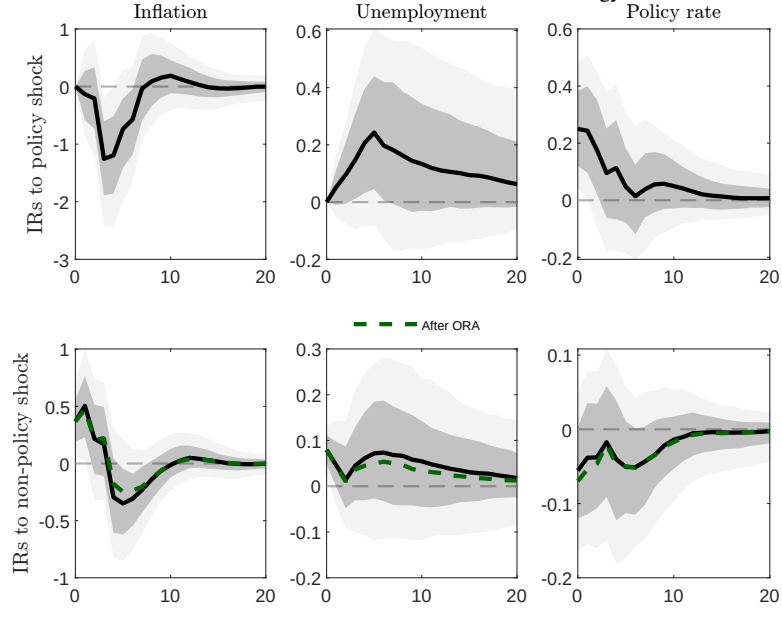

Note: The top row shows the median responses (thick line) of inflation, unemployment and the policy rate to a monetary policy shock. The bottom row shows the median responses (thick line) of inflation, unemployment and the policy rate to an energy price shock. The dotted green lines show the ORA adjusted impulse responses $\Gamma_0^0 + \mathcal{R}_0^0 \tau_0^*$. The 95% and 68% credible sets are plotted as dark and light shaded areas, respectively.

FIGURE S14.— Early Fed, 1913-1941, Reaction to Energy shocks

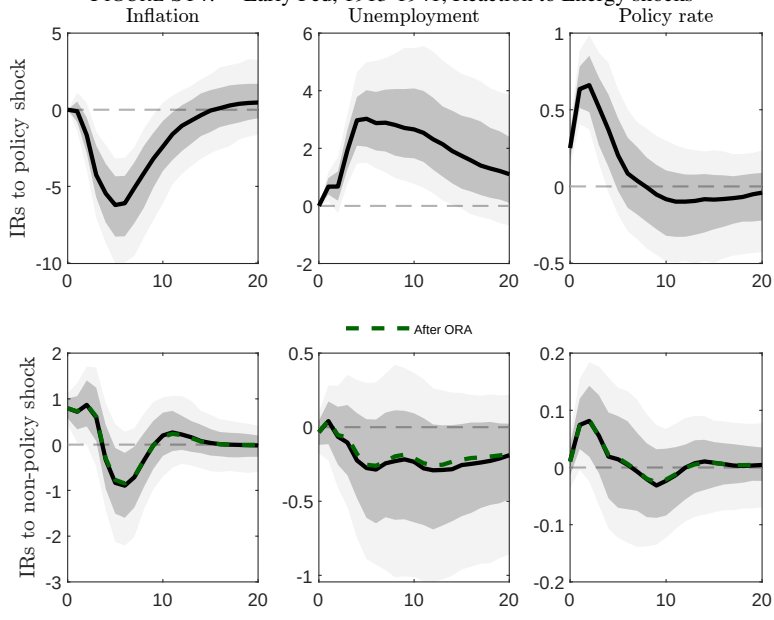

FIGURE S15.— Post WWII Fed, 1951-1984, Reaction to Energy shocks

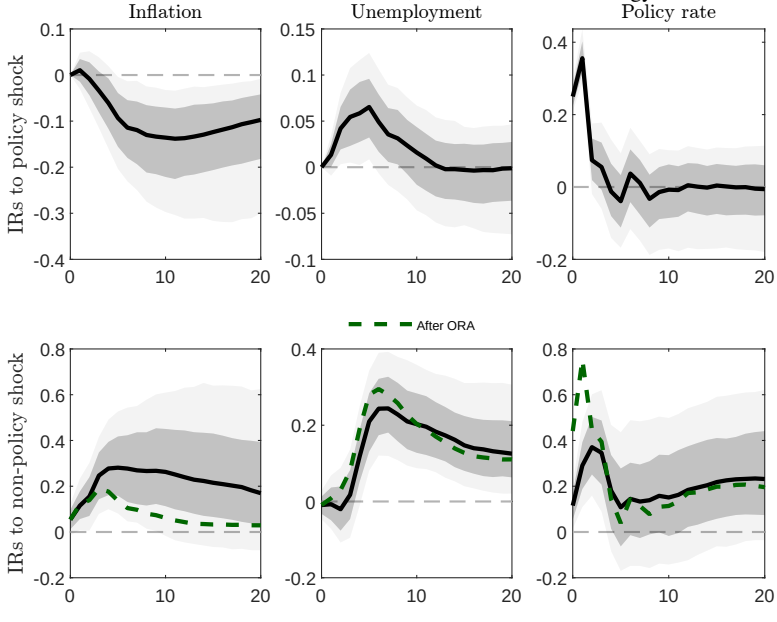

Note: The top row shows the median responses (thick line) of inflation, unemployment and the policy rate to a monetary policy shock. The bottom row shows the median responses (thick line) of inflation, unemployment and the policy rate to an energy price shock. The dotted green lines show the ORA adjusted impulse responses $\Gamma_0^0 + \mathcal{R}_0^0 \tau_0^*$. The 95% and 68% credible sets are plotted as dark and light shaded areas, respectively.

FIGURE S16.— Post Volcker Fed, 1990-2019, Reaction to Energy shocks

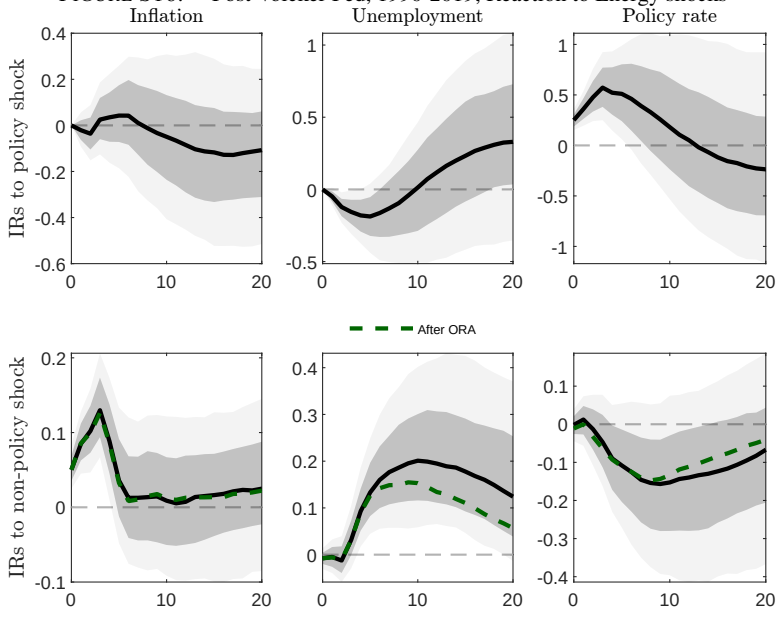

FIGURE S17.— Early Fed, 1913-1941, Reaction to π^e shocks

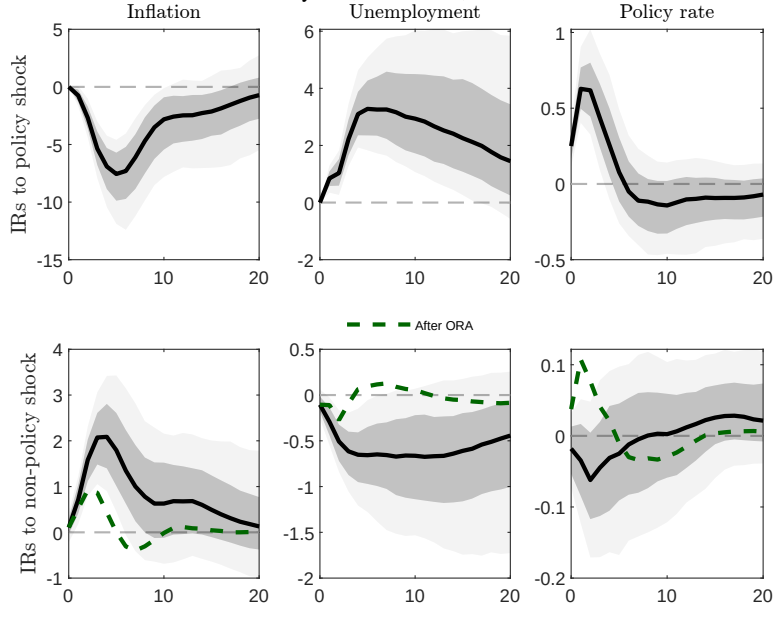

FIGURE S18.— Post WWII Fed, 1951-1984, Reaction to π^e shocks

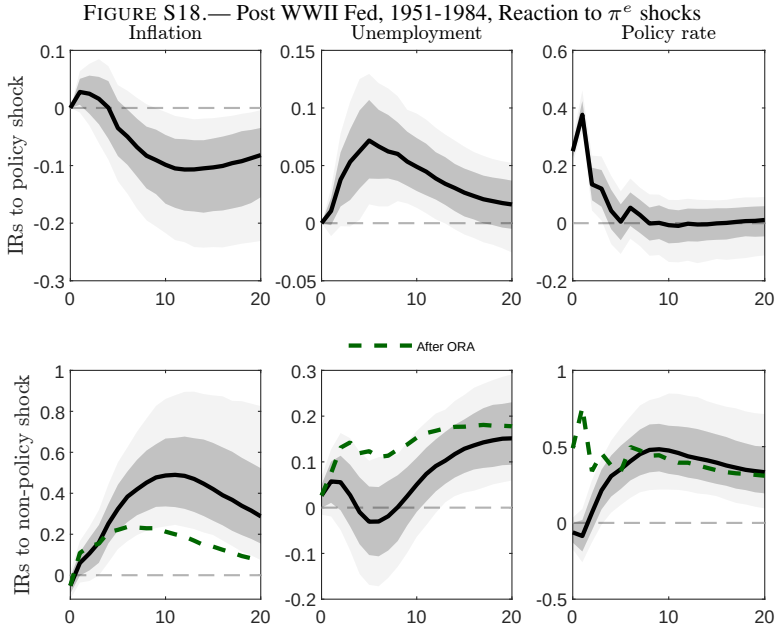

Note: The top row shows the median responses (thick line) of inflation, unemployment and the policy rate to a monetary policy shock. The bottom row shows the median responses (thick line) of inflation, unemployment and the policy rate to an inflation expectation shock. The dotted green lines show the ORA adjusted impulse responses $\Gamma_0^0 + \mathcal{R}_0^0\tau_0^*$. The 95% and 68% credible sets are plotted as dark and light shaded areas, respectively.

FIGURE S19.— Post Volcker Fed, 1990-2019, Reaction to π^e shocks

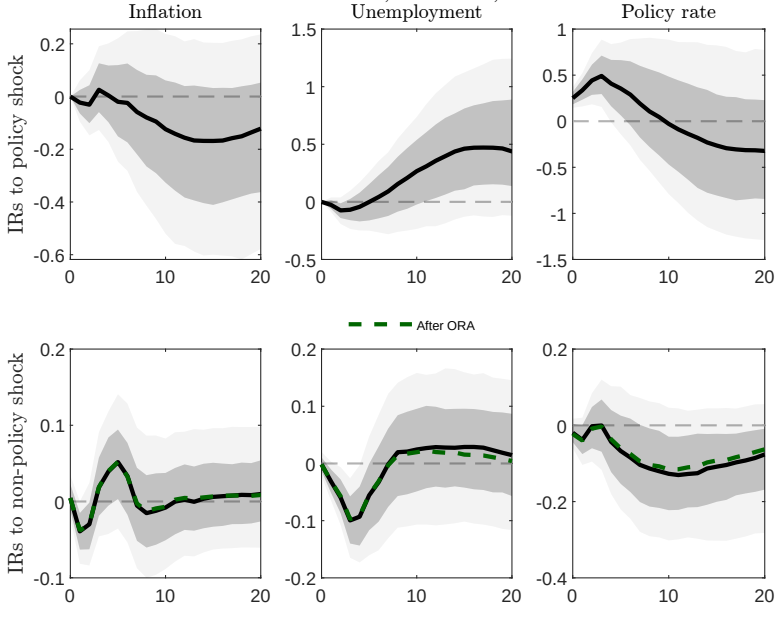

Note: The top row shows the median responses (thick line) of inflation, unemployment and the policy rate to a monetary policy shock. The bottom row shows the median responses (thick line) of inflation, unemployment and the policy rate to an inflation expectation shock. The dotted green lines show the ORA adjusted impulse responses $\Gamma_0^0 + \mathcal{R}_0^0\tau_0^*$. The 95% and 68% credible sets are plotted as dark and light shaded areas, respectively.

FIGURE S20.— Post WWII Fed, 1951-1984, Reaction to TFP shocks

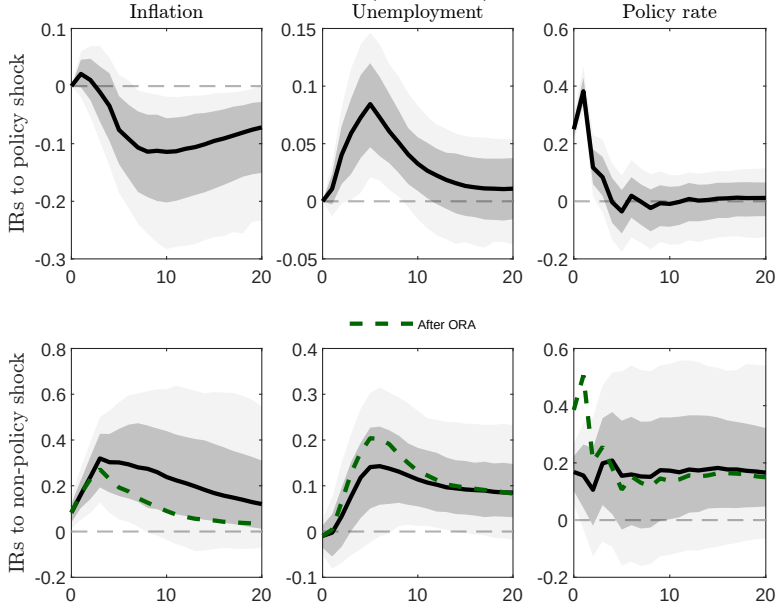

FIGURE S21.— Post Volcker Fed, 1990-2019, Reaction to TFP shocks

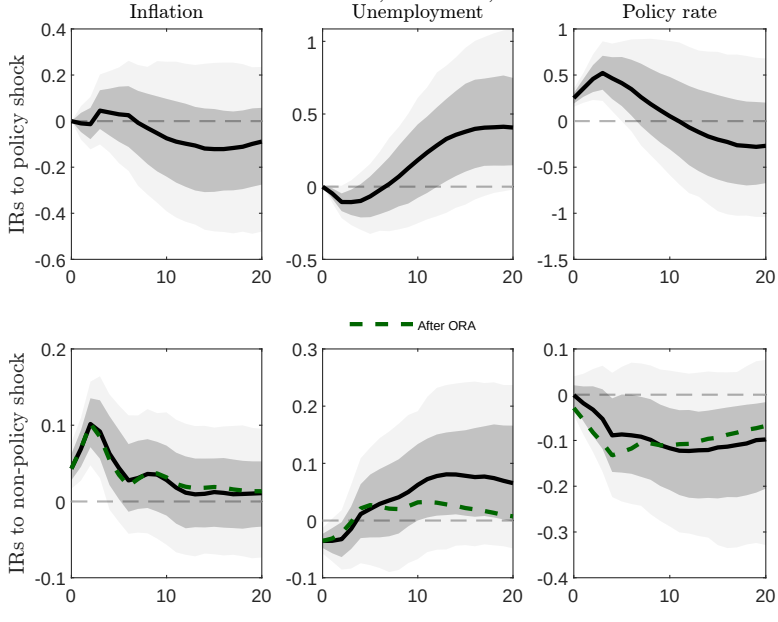

Note: The top row shows the median responses (thick line) of inflation, unemployment and the policy rate to a monetary policy shock. The bottom row shows the median responses (thick line) of inflation, unemployment and the policy rate to a TFP shock. The dotted green lines show the ORA adjusted impulse responses $\Gamma_0^0 + \mathcal{R}_0^0 \tau_0^*$. The 95% and 68% credible sets are plotted as dark and light shaded areas, respectively.